www.sciencemag.org/content/344/6190/1384/suppl/DC1

Supplementary Materials for

Controlling low rates of cell differentiation through noise and ultrahigh feedback

Robert Ahrends, Asuka Ota, Kyle M. Kovary, Takamasa Kudo, Byung Ouk Park, Mary N. Teruel*

*Corresponding author. E-mail: mteruel@stanford.edu

Published 20 June 2014, *Science* **344**, 1384 (2014)
DOI: 10.1126/science.1252079

This PDF file includes:

Controlling low rates of terminal cell differentiation through noise and ultra-high feedback in the signaling system

Supplementary information

Materials and Methods

LC-MS setups

A Proxeon nanospray ionization source was used as an interface between an EASY-nLC Nano-HPLC system (Proxeon, Odense, Denmark) and a TSQ Vantage triple quadrupole MS system (Thermo Fisher Scientific, Bremen, Germany). The peptide separation was carried out using a 25 mm x 0.1 mm C18 trapping column (MICHROM C18, 5 µm, 120 Å) and a 200mm x 0.075 mm diameter reverse-phase C18 capillary column (Maisch C18, 3µm, 120 Å). Peptides (up to 4µg of total protein digest) were separated with a linear gradient from 0% to 45% acetonitrile in 70 min, at a flow rate of 300 nl/min. For MS experiments, the following mode and tuning parameters were used: Polarity: positive, for scheduled SRM a maximum window of 5 min, a cycle time of 1s and an average dwell time of 26 ms was used for scheduled analysis, Q1 and Q3 were set to 0.70 u (FWHM), emitter voltage was set to 1500 V and the temperature of the transfer capillary to 270°C.

For all MS runs, standard LC/ESI SRM analysis were performed regularly using a digested six *Bos taurus* protein standard mixture (MICHROM, USA) to ensure best possible instrument performance.

Sample Preparation for Mass Spectrometry Analysis

In order to be able to measure small changes in protein concentration between different samples, great pains were taken to make the sample preparations as consistent and reproducible as possible. Cells were pelleted by a low-speed spin, washed one time with PBS followed by a low-speed spin and aspiration, and frozen in liquid nitrogen. To extract proteins, the frozen pellet was first thawed on ice and then resuspended in 100 µl per million cells of ice-cold lysis buffer consisting of 10 mM Hepes (pH 7.9), 1.5 mM $MgCl_2$, 10 mM KCl, 1 mM DTT, 0.01% digitonin, 1 mM PMSF, and a complete protease inhibitor cocktail (Roche, Mannheim, Germany). Cells were broken open by triturating 3 times through a 25-gauge needle and syringe and 3 times through a 30-gauge needle and syringe. The cell lysate was centrifuged at 2,300g for 10 min to pellet the nuclei, the supernatant represents the cytosolic and membrane fraction. Nuclei were washed by resuspending in 30ul per million cells of digitonin-free lysis buffer, spinning at 2,300g for 10 min at 4°C, and discarding the supernatant. Nuclear pellets were resuspended in a high salt buffer consisting of 20mM Hepes (pH 7.9), 25% v/v glycerol, 450 mM KCl, 1.5 mM $MgCl_2$, 0.2mM EDTA, 1mM DTT, 1 mM PMSF, and a complete protease inhibitor cocktail to extract the soluble nuclear protein fraction. Samples were placed on ice for 15 minutes followed by gentle shaking every 5 minutes for 15 minutes before centrifuging at 16,100 g for 10 minutes to pellet out the histones, which were dissolved in 8M urea for further use. The nuclear proteins in the supernatant were precipitated by adding 3 sample volumes of ice-cold acetone, storing overnight at -20°C, and then centrifuging at 16,100g to pellet the precipitated nuclear proteins. To obtain the cytosolic fraction the membranes were pelleted at 70,000 rpm (Beckmann Optima XL) and the supernatant subjected to acetone precipitated as described before the efficiency of the fractionation protocol is displayed in Fig. S4.

The pellets (nucleus, cytosolic, histone) were dissolved in 8M urea, and then the 8M urea solution was diluted down to 2M urea with 50 mM ammonium bicarbonate to enable the use of a BCA kit (Thermo Fischer Scientific, USA) to measure the concentration of the proteins in each sample. The BCA readings were used to measure the total protein concentration of each sample in order to make the subsequent addition of heavy peptides and trypsin as accurate as possible. The disulfide bonds of the proteins were reduced by incubation with tris(2-carboxyethyl)phosphine (TCEP) at a final concentration of 10 mM for 30 minutes at 37 °C. The produced free thiol groups were alkylated with 15 mM iodoacetamide (Sigma Aldrich, USA) at room temperature for 30 minutes in the dark before the samples were diluted to 1M urea with 50 mM ammonium bicarbonate. The heavy peptide mix was prepared as described below, and a protein amount based volume of 1 µl (130 femtomol/ 1 µg protein) was added to each sample. Sequencing-grade modified trypsin (Promega, Cat #V5113) was added at a ratio of 1 µg per 100 µg of protein, and the proteins were digested overnight at 37°C. The peptides were acidified to pH 2-3 with formic acid, desalted on a C18 Sep-Pak cartridge (Waters, Milford, MA, USA), and evaporated on a lyophilizer. The peptides were resolubilized in 2% acetonitrile with 0.1% formic acid. The concentration of peptides in each sample was read out at 230 nm using a Nanodrop (Thermo Fischer Scientific, USA) to ensure that the same amount of sample is injected for separation and SRM analysis.

Peptide and SRM Transition Selection

The workflow for developing SRM assays is shown in Fig. S3. Proteotypic peptides and transitions (precursor/fragment ions) were selected primarily by screening through the entire sequence of the target protein using unscheduled LC/ESI SRM analysis with the following SRM

setup: a scan width of 0.002 m/z was used and a scan time 0.02 s was applied, Q1 and Q3 were set to 0.70 FWHM and the collision gas pressure was of 1.5 Torr. After a set of high quality transitions were found for a peptide (more than 4 transitions that each had a S/N > 3), the set was validated by using a heavy-labeled synthetic version of each peptide. The heavy peptides were obtained from JPT Peptides (Berlin, Germnay) and were isotopically-labeled, ensuring that they co-eluted exactly with the endogenous peptides and the peak areas could be directly ratioed. In each peptide the C-terminal amino acid K or R residue was substituted with the corresponding heavy version resulting in a mass shift of +8 Da or +10 Da, respectively. The heavy internal standard peptides were tested to confirm that their light background showed no or almost no contaminating background (less than 1:10000, Fig. S5).

If the endogenous and the heavy-labeled internal standard peptides showed the same retention time and fragment ion intensity distribution during collision induced fragmentation, the endogenous peptides was used as protein probe. Finally we chose between two (high abundant proteins) to seven (for low abundant protein) transitions with the best signal/noise ratio and optimized the collision energy for best sensitivity (Fig. S6). The validated and optimized SRM transitions were used to detect and/or quantify the proteins in nuclei lysates using scheduled SRM mode. By restricting the acquisition of each transition to 2.5 minutes around its elution time, the time-scheduling feature of the acquisition software enabled the analysis of the 696 transitions in a single run per sample with high sensitivity. Table S2 shows the list of targeted peptides and transitions. To further validate the found peptide probes for proteins which had a regulatory effect on PPARG or vice versa, an siRNA knockdown experiment was performed (Fig. S7). For this purpose, the samples were collected during differentiation at the timepoint where the siRNA targeted protein was expressed maximally during normal differentiation. The

samples were then analyzed by SRM mass spectrometry and compared to a YFP siRNA treated control.

SRM-based quantification

For quantitative analysis, a heavy, isotopically-labeled synthetic version of each peptide of interest was custom ordered from JPT Peptides (Berlin, Germany). The heavy peptides were solubilized in 50 µl of a 20% ACN, 50 mM ammonium bicarbonate solution and combined to a final concentration of 1.6 µM. The peptide transitions in heavy and light versions were measured using scheduled SRM. SRM traces were analyzed using Skyline version 2.0 software (Maccoss lab, U. Washington). Peak areas for the transitions associated with the heavy and light peptides were quantified by ratioing light and heavy peptide areas. Furthermore the potential contamination of the heavy peptide preparations with the corresponding unlabeled peptides was investigated by injecting the heavy peptides alone (1 pmol) and monitoring the transitions for both the heavy and light peptide forms. At the concentration used for quantitative measurements no signal heavy signal was detectable in the ‘‘light’’ transitions (Fig. S5). In order to detect unexpected dramatic sample losses occurring during sample preparation several standard proteins were monitored during time course of adipogenesis, the different siRNA and chemical perturbations experiments. The following proteins HNRNPAB, HNRNPA2B1, CSTF3, SFRS1, SF3B3 and CREB1 were used as controls to ensure that no major sample loss in one of the biological replicates occurred or the whole experiment was affected by external factors. Samples which showed major discrepancies in-between the biological replicates and/or measuring points were excluded. The results were calculated by ratioing the areas between the light and heavy peptides. For every data point, 3 independent biological samples were analyzed and the error was

calculated as the standard deviation of the mean. All timepoint SRM data were normalized to day 0. All data obtained from the rosiglitazone titration experiment were normalized to the highest concentration point if they were rising and to the lowest drug concentration if they were dropping during rosiglitazone titration.

Cell culture and differentiation

OP9 cells were cultured according to the protocols in Wollins et al. (23). OP9 cells were cultured in growth media consisting of MEM-α (GIBCO, # 12561-056), 100 units/mL Penicillin, 100µg/mL Streptomycin, and 292 µg/mL L-glutamate (Gibco, # 10378-016). To differentiate, 5 million OP9 cells were plated in T75 flasks in growth media plus 20% FBS. The following day, the media on the cells was replaced with growth media plus 10% FBS, 0.517 mM IBMX (Sigma Aldrich, USA), and 62 nM dexamethasone (Sigma Aldrich, USA) (Stimulus I). After two days, Stimulus I was removed from the cells and was replaced with Stimulus II consisting of growth media plus 10% FBS and 172 nM insulin (Sigma Aldrich, USA) for two more days (Fig. S9).

Immunofluorescence Staining

OP9 cells were fixed with 3% paraformaldehyde in PBS for 30 min. Then the cells were gently washed 3X with PBS and permeabilized with 0.05% saponin (Sigma #47036), blocked with 3% bovine serum albumin (Sigma #7906) and stained with DAPI (1:10000), anti-PPARG (1:500 Santa Cruz Biotech #sc-7273), anti-CEBPA (1:500, Santa Cruz Biotech #sc-61), anti-CEBPB (1:500, Santa Cruz Biotech #sc-150), anti-CEBPA (1:500, Santa Cruz Biotech #sc-7962) or BODIPY 493/503, (1µg/ml, Molecular Probes #D-3922). Alexa Fluor-514 (#A31558), 555

(#A21429), 594 (#A11032) and 647 (#A31571) (1:1000, Invitrogen) were used as secondary antibodies (Fig. S9).

Drug treatments

For the drug treatments the same media and conditions were used as described before with the following exceptions: A quarter of Stimulus I was used with either 10 µM rosiglitazone (Cayman, USA) or 0.5 µM CHIR-99021 (Cayman, USA). For the rosiglitazone titration no IBMX, dexamethasone or insulin was used. Rosiglitazone was titrated from 0 to 0.5 µM, and the cells were pelleted after 48 hours. The rosiglitazone time course experiment was carried out with 10 µM rosiglitazone in 10% FBS MEM-alpha and the cells were pelleted after 0, 1.5, 3, 6, 12, 24, 36, 48, 72 and 96 hours of differentiation. All experiments were performed in triplicates.

siRNA preparation and transfection

Diced pool siRNA was generated as described previously (*7*, *30*). Gene-specific primers were designed with an in-house primer program and were used to generate ~600 bp cDNA fragments immediately upstream of the stop codon of each mRNA by PCR. An additional set of nested primers were designed to add T7 promoters at both ends of the final cDNA fragment. Table S3 shows a list of all primers used to make the siRNA. Nested PCR products were subjected to *in vitro* transcription, *in vitro* dicing, and purification to produce siRNA. OP9 cells were transfected with siRNA by a reverse transfection protocol. For each 96-well well, 2 pmol of diced-pool siRNA were diluted in 10µl of Opti-Mem I Medium. 0.2µl of RNAiMax (Invitrogen) diluted in 10µl of Opti-Mem I was then added, mixed well, and then incubated for 10 minutes at room temperature. This mixture was then placed into a 96-well, and OP9 cells were added

(15,000 cells suspended in 80 µl of growth medium without antibiotics). After 24 hours, the media was replaced with differentiation media to induce differentiation. For the siRNA experiments in T75 flasks the experiments were up scaled by the factor of 200 and carried out as described above. The knockdown efficiency for proteins found in feedback was further validated by SRM analysis (Fig. S7).

Automated image acquisition and processing

Images were acquired on an ImageXpress 5000A automated epifluorescence microscope (Molecular Devices; Sunnyvale, CA, USA) using a 4X Plan Fluor objective and a 1280 × 1024 pixel, cooled CCD camera with a 12-bit readout. Image analysis was performed using custom software written in Matlab. In brief, nuclear centroids were identified in images of Hoechst stain. A nucleus mask was generated for each cell by expansion from the centroid to reach 30% off maximum intensity. A cell mask was then generated by expansion of the nucleus mask 7 µm to include both the nucleus and the perinuclear region. After local background subtraction, the nucleus mask was used to measure PPARG, C/EBPB mean intensities, and the cell mask was used to measure BODIPY (lipid droplet content).

Defining differentiation

We have previously shown that the transition from a proliferating preadipocyte precursor cell into a mature, non-proliferating adipocyte capable of accumulating lipid occurs via a bistable switch from low PPARG expression in the cell to high PPARG expression (7). As shown in Fig. 1A, a histogram of PPARG expression for a population of differentiating adipocytes shows two peaks of PPARG expression - low and high. The high state predicts the subsequent lipid droplet

formation. We thus define a cell as being differentiated if its level of PPARG placed the cell in the high PPARG-expressing peak of the cell population.

Calculating overall cooperativity of the system

Model 2 in Fig.2 depicts a system with 6 positive feedback loops, each with a cooperativity of 2 (Model 2 in Fig. 2). If the 6 feedback loops are working as AND-gates, their contributions should be multiplied together, and the system can be described with the following equations:

$$\frac{dX_0}{dt} = \varepsilon_0 * R * \left(1 + \alpha * \frac{X_1^2 * X_2^2 * X_3^2 * X_4^2 * X_5^2 * X_6^2}{1 + X_1^2 * X_2^2 * X_3^2 * X_4^2 * X_5^2 * X_6^2} \right) - X_0 \quad (1)$$

$$\frac{dX_j}{dt} = \varepsilon_j * X_0 - X_j \quad \text{where} \quad j = 1,...,6 \quad (2)$$

In the steady-state, eqn (2) becomes:

$$X_1 = \varepsilon_1 * X_0$$

$$\vdots$$

$$X_6 = \varepsilon_6 * X_0$$

Plugging into eqn (1):

$$0 = \varepsilon_0 * R * \left(1 + \alpha * \frac{\varepsilon_1 X_0^2 * \varepsilon_2 X_0^2 * \varepsilon_3 X_0^2 * \varepsilon_4 X_0^2 * \varepsilon_5 X_0^2 * \varepsilon_6 X_0^2}{1 + \varepsilon_1 X_0^2 * \varepsilon_2 X_0^2 * \varepsilon_3 X_0^2 * \varepsilon_4 X_0^2 * \varepsilon_5 X_0^2 * \varepsilon_6 X_0^2} \right) - X_0$$

$$0 = \varepsilon_0 * R * \left(1 + \alpha * \frac{\left(\varepsilon_1 \varepsilon_2 \varepsilon_3 \varepsilon_4 \varepsilon_5 \varepsilon_6\right) * \left(X_0^2 X_0^2 X_0^2 X_0^2 X_0^2 X_0^2\right)}{1 + \left(\varepsilon_1 \varepsilon_2 \varepsilon_3 \varepsilon_4 \varepsilon_5 \varepsilon_6\right) * \left(X_0^2 X_0^2 X_0^2 X_0^2 X_0^2 X_0^2\right)} \right) - X_0$$

$$0 = \varepsilon_0 * R * \left(1 + \alpha * \frac{\left(\varepsilon_1 \varepsilon_2 \varepsilon_3 \varepsilon_4 \varepsilon_5 \varepsilon_6\right) * X_0^{12}}{1 + \left(\varepsilon_1 \varepsilon_2 \varepsilon_3 \varepsilon_4 \varepsilon_5 \varepsilon_6\right) * X_0^{12}} \right) - X_0$$

Thus, this system has a cooperativity of n=12.

If feedback loops are in an OR-gate configuration, the feedback loop contributions could replace each other, and in this case we would add the contributions. For example, if feedback loops to proteins X1 through X4 served as AND-gates and X5 and X6 were OR-gates, the equations would be as follows:

$$\frac{dX_0}{dt} = \varepsilon_0 * R * \left(1 + \alpha * \frac{X_1^2 * X_2^2 * X_3^2 * X_4^2 + X_5^2 + X_6^2}{1 + X_1^2 * X_2^2 * X_3^2 * X_4^2 + X_5^2 + X_6^2} \right) - X_0 \quad (3)$$

$$\frac{dX_j}{dt} = \varepsilon_j * X_0 - X_j \quad \text{where} \quad j = 1,...,6 \tag{4}$$

We initially assumed that the network topology included AND-gates because we had already identified two such AND-gates (CEBPA and CEBPB) in the network in a previous study by showing that knocking these proteins down individually with siRNA indeed killed the entire network response (7).

In the current study, we confirmed experimentally for at least four of the positive feedback loops - CEBPA, CEBPB, FAPB4, and LPIN1- that they must be configured during adipogenesis as AND-gates. siRNA-mediated depletion of each of these feedback loop proteins individually results in a near complete lack of adipogenesis in most cells (enrichment of cells in the low PPARG abundance peak as marked by the solid lines, top two plots on left, Fig. 4C). In addition, CEBPA and FABP4 are connected to the network as AND-gates during de-differentiation as demonstrated by the fact that siRNA-mediated depletion of these feedback loop proteins individually under de-differentiation conditions results in a near complete loss of PPARG expression in many cells (solid lines, top right plot, Fig. 4C).

In the current study, we identified 4 positive-loops in an AND-gate configuration based on this criterion. A more complete knockdown in expression than is attainable by siRNA may show that the other 3 loops identified in this study may also have at least a partial AND-configuration.

The specific connection mechanism by each of the different feedback loops is likely not the same and may include different cooperativities, time constants, as well as mixtures of additive (OR-gate) and multiplicative (AND-gate) features. Since the precise wiring structure of a complex network is difficult to dissect, we are simplifying the likely mixture of AND and OR features by defining a feedback loop protein as being connected as an AND-gate if the protein is required for adipogenesis (the knockdown kills differentiation). In general, increasing the relative fraction of additive (OR-gate) regulatory feedback loops loops (compared to multiplicative AND-gate loops) confers less of a benefit for balancing low differentiation rates and keeping the system in the locked differentiated state.

The individual feedbacks may also vary in their half-maximal response values; in other words, each feedback loop may kick ‘on’ at a different threshold concentration of its respective transcription factor, which would confound the simple additivity of the Hill coefficients and the overall response.

Calculation of errors (for more details, see (*31*))

The uncertainty in a sum $q = x + y$ or a product $q = x * y$ is: $\delta q = \delta x + \delta y$

If $q = x^n$, the uncertainty then is: $\Delta q \sim |n| * \Delta x$

However, when the uncertainties in a sum $q = x + y$ or a product $q = x * y$ are independent and random, the uncertainties are added in quadrature: $\Delta q \sim \sqrt{\Delta x^2 + \Delta y^2}$

The equations for a one feedback loop system with a cooperativity of 12 (Model 1 in Fig. 2) are:

$$\frac{dX_0}{dt} = \varepsilon_0 * R * \left(1 + \alpha * \frac{X_1^{12}}{1 + X_1^{12}}\right) - X_0$$

$$\frac{dX_1}{dt} = \varepsilon_1 * X_0 - X_1$$

where $\varepsilon_0 \cong \varepsilon_1 \cong 30\%$ log normal noise

The feedback amplification, $\alpha = 15$, reflects the increase in PPARG expression measured experimentally in (7).

In the undifferentiated, basal state where the feedback-induced noise is low:

$$\frac{dX_0}{dt} = \varepsilon_0 * R_0$$

In the transition region where the feedback loops are fully engaged and the feedback-induced noise dominates:

$$\frac{dX_0}{dt} = \varepsilon_0 * R * \alpha * X_1^{12} \sim \varepsilon_0 * R * \alpha * \varepsilon_1^{12} X_0^{12}$$

$$\sim \sqrt{\varepsilon_0^2 + \left(\varepsilon_1^{12}\right)^2} \text{ since } \varepsilon_0 \text{ and } \varepsilon_1 \text{ are independent}$$

The error is then $\sim \varepsilon_1^{12} \sim \varepsilon_0^{12} \sim 12 * \varepsilon_0$

The equations for a six feedback loop system with a total cooperativity of 12 in which each loop has a cooperativity of 2 (Model 2 in Fig. 2) are:

$$\frac{dX_0}{dt} = \varepsilon_0 * R * \left(1 + \alpha * \frac{X_1^2 * X_2^2 * X_3^2 * X_4^2 * X_5^2 * X_6^2}{1 + X_1^2 * X_2^2 * X_3^2 * X_4^2 * X_5^2 * X_6^2} \right) - X_0$$

$$\frac{dX_j}{dt} = \varepsilon_j * X_0 - X_j \quad \text{where} \quad j = 1,...,6$$

In the undifferentiated, basal state where the feedback-induced noise is low:

$$\frac{dX_0}{dt} \sim \varepsilon_0 * R_0$$

In the transition region where the feedback loops are fully engaged and the feedback-induced noise dominates:

$$\frac{dX_0}{dt} \sim \varepsilon_0 * R * \alpha * X_1^2 * X_2^2 * X_3^2 * X_4^2 * X_5^2 * X_6^2$$

$$\sim \varepsilon_0 * R * \alpha * \varepsilon_1^2 X_0^2 * \varepsilon_2^2 X_0^2 * \varepsilon_3^2 X_0^2 * \varepsilon_4^2 X_0^2 * \varepsilon_5^2 X_0^2 * \varepsilon_6^2 X_0^2$$

Assuming that $\varepsilon_0 \sim \varepsilon_n \sim 30\%$ log normal noise ,

the error would be $\sim \sqrt{\varepsilon_0 + (2 * \varepsilon_1)^2 + (2 * \varepsilon_2)^2 + (2 * \varepsilon_3)^2 + (2 * \varepsilon_4)^2 + (2 * \varepsilon_5)^2 + (2 * \varepsilon_6)^2}$

$$\sim \sqrt{\varepsilon_0 + (2 * \varepsilon_0)^2 + (2 * \varepsilon_0)^2 + (2 * \varepsilon_0)^2 + (2 * \varepsilon_0)^2 + (2 * \varepsilon_0)^2}$$

$$\sim \sqrt{\varepsilon_0^2 + 6 * 4 * \varepsilon_0^2} \quad \text{since the errors are all independent}$$

$$\sim 4.9 * \varepsilon_0$$

The noise is likely bigger in the synthesis versus degradation rates of the proteins in the system since mRNA copy number is believed to be the significant source of noise in mammalian cells (16). Thus, in the current simulations, all error terms were added to the protein synthesis rates. However, mathematically the results should be similar if noise is attributed to both protein synthesis and degradation rates. In practice, noise is added to each simulation by calculating a normally-distributed random variable that is then converted to a log scale and multiplied with the synthesis rate to give a relative error.

Calculation of differentiation rate:

~10% of adipocytes are turned over every year in human adults (*6*)

If it takes ~ 4 days for adipocytes to differentiate from preadipocytes (3):

365 days per year/ 4 days to differentiate ~ 91.25 time periods during the year in which to differentiate

With a 10% yearly turnover divided by 91.25 time periods per year in which to differentiate ~0.1% of adipocytes are differentiating at any given time. Thus humans cannot lose more than ~0.1% of their adipocytes if they want to maintain their current fat mass.

Since there are ~5 adipocytes to 1 preadipocyte (2), ~0.5% of preadipocytes (or 1 preadipocyte out of 200) must be differentiating at any given time.

If it takes ~ 12 days for adipocytes to differentiate from preadipocytes:

365 days per year/ 12 days to differentiate ~ 30.4 time periods during the year in which to differentiate

With a 10% yearly turnover divided by 30.4 time periods per year in which to differentiate ~0.33% of adipocytes are differentiating at any given time. Thus humans cannot lose more than ~0.33% of their adipocytes if they want to maintain their current fat mass.

Since there are ~5 adipocytes to 1 preadipocyte (2), ~1.65% of preadipocytes (or 1 preadipocyte out of 60) must be differentiating at any given time

---

Thus, if it takes between 4-12 days for a preadipocyte to differentiate into an adipocyte, between 0.5-1.65 % of preadipocytes must be differentiating at any given time.

Table S1: List of monitored proteins.

No	*Protein*	*NP*	*Description*
1	NFIL3	NP_059069.1	Nuclear factor interleukin-3-regulated protein
2	FOXK1	NP_951031.2.	Forkhead box protein K1
3	CREB1	NP_598589.2.	Cyclic AMP-responsive element-binding protein 1
4	SIRT2	NP_001116237.1.	NAD-dependent deacetylase sirtuin-2
5	SCMARCA5	NP_444354.2	SWI/SNF related, matrix associated, actin dependent regulator of chromatin, subfamily a, member 3
6	SMARCA4	NP_035547.1	SWI/SNF related, matrix associated, actin dependent regulator of chromatin, subfamily a, member 4
7	SMARCC1	NP_033237.2	SWI/SNF related, matrix associated, actin dependent regulator of chromatin, subfamily c, member 1
8	SMARCC2	NP_444354.2.	SWI/SNF-related matrix-associated actin-dependent regulator of chromatin subfamily A member 5
9	SMARCE1	NP_065643.1.	SWI/SNF-related matrix-associated actin-dependent regulator chromatin subfamily E member 1
10	SMARCD2	NP_001123659.1	SWI/SNF related, matrix associated, actin dependent regulator of chromatin, subfamily d, member 2
11	MGMT	NP_032624.1.	Methylated-DNA--protein-cysteine methyltransferase
12	BRD8	NP_084423.2.	Bromodomain-containing protein 8
13	TRIM28	NP_035718.2.	Transcription intermediary factor 1-beta
14	WDR5	NP_543124.1.	WD repeat-containing protein 5
15	MYBBP1a	NP_058056.2	myb-binding protein
16	PPARG	NP_001120802.1.	peroxisome proliferator-activated receptor gamma
17	CEBPA	NP_031704.2	CCAAT/enhancer-binding protein alpha
18	CEEBPB	NP_034013.1	CCAAT/enhancer-binding protein beta
19	CEBPZ	NP_001019977.1	CCAAT/enhancer-binding protein zeta
20	EEF1A1	NP_034236.2.	Elongation factor 1-alpha 1
21	FABP4	NP_077717.1.	Fatty acid-binding protein, adipocyte
22	FLNA	NP_034357.2	Alpha-filamin Endothelial actin-binding protein
23	FOXC2	NP_038547.2.	Forkhead box protein C2
24	APEX1	NP_033817.1.	DNA-(apurinic or apyrimidinic site) lyase
25	CSTF3	NP_663504.1.	Cleavage stimulation factor subunit 3
26	SF3B3	NP_598714.1.	Pre-mRNA-splicing factor SF3b
27	NONO	NP_075633	Non-POU domain-containing octamer-binding protein
28	HNRNPA2b1	NP_058086.2.	Heterogeneous nuclear ribonucleoproteins A2/B1
29	SFRS1	NP_001071635.1.	Serine/arginine-rich splicing factor 1
30	HNRNPAB	NP_034578.1.	Heterogeneous nuclear ribonucleoprotein A/B
31	POLR2H	NP_663607.1.	DNA-directed RNA polymerases I, II, and III subunit RPABC3
32	UBAP2L	NP_001159455.1.	Ubiquitin-associated protein 2-like

33	NEDD4	NP_035020.2.	E3 ubiquitin-protein ligase NEDD4
34	CSRP1	NP_031817.1.	Cysteine and glycine-rich protein 1
35	PTBP1	NP_001070831.1	polypyrimidine tract binding protein
36	ACTL6A	NP_062647.2.	Actin-related protein Baf53a
37	BAZ1B	NP_035844.2.	Bromodomain adjacent to zinc finger domain protein 1B
38	BCLAF	NP_001020563.1.	Bcl-2-associated transcription factor 1
39	CAND1	NP_082270.1.	Cullin-associated NEDD8-dissociated protein 1
40	CTBP1	NP_001185788.1.	C-terminal-binding protein 1
41	CTBP2	NP_001164215.1.	C-terminal-binding protein 2
42	DCUN1	NP_001192290.1.	Defective in cullin neddylation protein 1-like protein 1
43	MYH9	NP_071855.2.	Cellular myosin heavy chain, type A
44	ELAVL1	NP_034615.2.	ELAV-like protein 1
45	GSK3B	NP_062801.1.	Glycogen synthase kinase-3 beta
46	LMNA	NP_001002011.2.	Lmna Isoform C2
47	NFKB1	NP_032715.2.	Nuclear factor NF-kappa-B p105 subunit
48	NSUN2	NP_663329.3.	Myc-induced SUN domain-containing protein
49	RCOR1	NP_932140.1.	REST corepressor 1
50	TAX1BP3	NP_083840.1.	Tax1-binding protein 3
51	ZFP326	NP_061229.2.	DBIRD complex subunit ZNF326
52	AEBP1	NP_033766.2.	Adipocyte enhancer-binding protein 1
53	AKAP8	NP_062748.2.	A-kinase anchor protein 8
54	CTNND1	NP_001078917.1.	Catenin delta-1
55	EMERIN	NP_031953.1.	Stabilizes and promotes the formation of a nuclear actin cortical network
56	RAD50	IPI00108335	DNA repair protein RAD50
57	RUNX2	NP_001139510.1.	Runt-related transcription factor 2
58	RUVBL1	NP_062659.1.	49 kDa TATA box-binding protein-interacting protein
59	LPIN1	NP_001123884.1.	Fatty liver dystrophy protein
60	RUVBL2	NP_035434.1.	RuvB-like 2

Table S2: Monitored peptide transitions.

Protein	*Peptide*	*Q1 [m/z]*	*Q3 [m/z]*	*CID [eV]*	*fragment ion*	*isotope*
ACTL6A	LIANNTTVER*	565.8	719.4	19.9	y6	light
ACTL6A	LIANNTTVER*	565.8	605.3	19.9	y5	light
ACTL6A	LIANNTTVER*	565.8	504.3	19.9	y4	light
ACTL6A	LIANNTTVER*	570.8	729.4	19.9	y6	heavy
ACTL6A	LIANNTTVER*	570.8	615.3	19.9	y5	heavy
ACTL6A	LIANNTTVER*	570.8	514.3	19.9	y4	heavy
ACTL6A	QGGPTYYIDTNALR	784.9	965.5	26.5	y8	light
ACTL6A	QGGPTYYIDTNALR	784.9	802.4	26.5	y7	light
ACTL6A	QGGPTYYIDTNALR	784.9	689.4	26.5	y6	light
ACTL6A	QGGPTYYIDTNALR	789.9	975.5	26.5	y8	heavy
ACTL6A	QGGPTYYIDTNALR	789.9	812.5	26.5	y7	heavy
ACTL6A	QGGPTYYIDTNALR	789.9	699.4	26.5	y6	heavy
ACTL6A	SPLAGDFITMQCR	748.4	1127.5	25.4	y9	light
ACTL6A	SPLAGDFITMQCR	748.4	808.4	25.4	y6	light
ACTL6A	SPLAGDFITMQCR	748.4	695.3	25.4	y5	light
ACTL6A	SPLAGDFITMQCR	753.4	1137.5	25.4	y9	heavy
ACTL6A	SPLAGDFITMQCR	753.4	818.4	25.4	y6	heavy
ACTL6A	SPLAGDFITMQCR	753.4	705.3	25.4	y5	heavy
BAZ1B	YQEITHSIYLAR*	747.4	960.5	25.3	y8	light
BAZ1B	YQEITHSIYLAR*	747.4	859.5	25.3	y7	light
BAZ1B	YQEITHSIYLAR*	747.4	722.4	25.3	y6	light
BAZ1B	YQEITHSIYLAR*	752.4	970.5	25.3	y8	heavy
BAZ1B	YQEITHSIYLAR*	752.4	869.5	25.3	y7	heavy
BAZ1B	YQEITHSIYLAR*	752.4	732.4	25.3	y6	heavy
BAZ1B	FSDFLLDPYK	622.8	748.4	21.6	y6	light
BAZ1B	FSDFLLDPYK	622.8	635.3	21.6	y5	light
BAZ1B	FSDFLLDPYK	622.8	522.3	21.6	y4	light
BAZ1B	FSDFLLDPYK	626.8	756.4	21.6	y6	heavy
BAZ1B	FSDFLLDPYK	626.8	643.4	21.6	y5	heavy
BAZ1B	FSDFLLDPYK	626.8	530.3	21.6	y4	heavy
Bclaf1	SPAVTLNER*	493.8	802.4	17.7	y7	light
Bclaf1	SPAVTLNER*	493.8	731.4	17.7	y6	light
Bclaf1	SPAVTLNER*	493.8	632.3	17.7	y5	light
Bclaf1	SPAVTLNER*	498.8	812.5	17.7	y7	heavy
Bclaf1	SPAVTLNER*	498.8	741.4	17.7	y6	heavy
Bclaf1	SPAVTLNER*	498.8	642.3	17.7	y5	heavy
CAND1	AVAALLTIPEAEK*	663.4	900.5	22.8	y8	light
CAND1	AVAALLTIPEAEK*	663.4	787.4	22.8	y7	light

CAND1	AVAALLTIPEAEK*	663.4	573.3	22.8	y5	light
CAND1	AVAALLTIPEAEK*	667.4	908.5	22.8	y8	heavy
CAND1	AVAALLTIPEAEK*	667.4	795.4	22.8	y7	heavy
CAND1	AVAALLTIPEAEK*	667.4	581.3	22.8	y5	heavy
CAND1	SVILEAFSSPSEEVK	811.4	862.4	27.2	y8	light
CAND1	SVILEAFSSPSEEVK	811.4	775.4	27.2	y7	light
CAND1	SVILEAFSSPSEEVK	811.4	688.4	27.2	y6	light
CAND1	SVILEAFSSPSEEVK	815.4	870.4	27.2	y8	heavy
CAND1	SVILEAFSSPSEEVK	815.4	783.4	27.2	y7	heavy
CAND1	SVILEAFSSPSEEVK	815.4	696.4	27.2	y6	heavy
CTBP1	IGSGFDNIDIK*	589.8	864.4	20.6	y7	light
CTBP1	IGSGFDNIDIK*	589.8	717.4	20.6	y6	light
CTBP1	IGSGFDNIDIK*	589.8	602.4	20.6	y5	light
CTBP1	IGSGFDNIDIK*	593.8	872.5	20.6	y7	heavy
CTBP1	IGSGFDNIDIK*	593.8	725.4	20.6	y6	heavy
CTBP1	IGSGFDNIDIK*	593.8	610.4	20.6	y5	heavy
CTBP1	QGAFLVNTAR	538.8	673.4	19.1	y6	light
CTBP1	QGAFLVNTAR	538.8	560.3	19.1	y5	light
CTBP1	QGAFLVNTAR	538.8	461.2	19.1	y4	light
CTBP1	QGAFLVNTAR	543.8	683.4	19.1	y6	heavy
CTBP1	QGAFLVNTAR	543.8	570.3	19.1	y5	heavy
CTBP1	QGAFLVNTAR	543.8	471.3	19.1	y4	heavy
CTBP1	VGQAVALR	407.3	714.4	15.1	y7	light
CTBP1	VGQAVALR	407.3	529.3	15.1	y5	light
CTBP1	VGQAVALR	407.3	458.3	15.1	y4	light
CTBP1	VGQAVALR	412.3	724.4	15.1	y7	heavy
CTBP1	VGQAVALR	412.3	539.4	15.1	y5	heavy
CTBP1	VGQAVALR	412.3	468.3	15.1	y4	heavy
CTBP2	IGSGYDNVDIK*	590.8	866.4	20.6	y7	light
CTBP2	IGSGYDNVDIK*	590.8	703.4	20.6	y6	light
CTBP2	IGSGYDNVDIK*	590.8	588.3	20.6	y5	light
CTBP2	IGSGYDNVDIK*	594.8	874.4	20.6	y7	heavy
CTBP2	IGSGYDNVDIK*	594.8	711.4	20.6	y6	heavy
CTBP2	IGSGYDNVDIK*	594.8	596.3	20.6	y5	heavy
CTBP2	QGAFLVNAAR	523.8	643.4	18.6	y6	light
CTBP2	QGAFLVNAAR	523.8	530.3	18.6	y5	light
CTBP2	QGAFLVNAAR	523.8	431.2	18.6	y4	light
CTBP2	QGAFLVNAAR	528.8	653.4	18.6	y6	heavy
CTBP2	QGAFLVNAAR	528.8	540.3	18.6	y5	heavy
CTBP2	QGAFLVNAAR	528.8	441.2	18.6	y4	heavy
DCUN1	SQLNDISSFK*	569.8	696.4	20	y6	light

DCUN1	SQLNDISSFK*	569.8	581.3	20	y5	light
DCUN1	SQLNDISSFK*	569.8	468.2	20	y4	light
DCUN1	SQLNDISSFK*	573.8	704.4	20	y6	heavy
DCUN1	SQLNDISSFK*	573.8	589.3	20	y5	heavy
DCUN1	SQLNDISSFK*	573.8	476.3	20	y4	heavy
CREB1	ILNDLSSDAPGVPR*	727.4	885.4	24.7	y9	light
CREB1	ILNDLSSDAPGVPR*	727.4	798.4	24.7	y8	light
CREB1	ILNDLSSDAPGVPR*	727.4	525.3	24.7	y5	light
CREB1	ILNDLSSDAPGVPR*	732.4	895.5	24.7	y9	heavy
CREB1	ILNDLSSDAPGVPR*	732.4	808.4	24.7	y8	heavy
CREB1	ILNDLSSDAPGVPR*	732.4	535.3	24.7	y5	heavy
Smarce1	IAAEIAQAEEQAR*	700.4	831.4	23.9	y7	light
Smarce1	IAAEIAQAEEQAR*	700.4	703.3	23.9	y6	light
Smarce1	IAAEIAQAEEQAR*	700.4	632.3	23.9	y5	light
Smarce1	IAAEIAQAEEQAR*	705.4	841.4	23.9	y7	heavy
Smarce1	IAAEIAQAEEQAR*	705.4	713.3	23.9	y6	heavy
Smarce1	IAAEIAQAEEQAR*	705.4	642.3	23.9	y5	heavy
MGMT	FGETVSYQQLAALAGNPK*	947.5	670.4	31.3	y7	light
MGMT	FGETVSYQQLAALAGNPK*	947.5	486.3	31.3	y5	light
MGMT	FGETVSYQQLAALAGNPK*	947.5	415.2	31.3	y4	light
MGMT	FGETVSYQQLAALAGNPK*	951.5	678.4	31.3	y7	heavy
MGMT	FGETVSYQQLAALAGNPK*	951.5	494.3	31.3	y5	heavy
MGMT	FGETVSYQQLAALAGNPK*	951.5	423.2	31.3	y4	heavy
MYBBP1a	QHFSFPLDDR*	631.3	996.5	21.8	y8	light
MYBBP1a	QHFSFPLDDR*	631.3	849.4	21.8	y7	light
MYBBP1a	QHFSFPLDDR*	631.3	615.3	21.8	y5	light
MYBBP1a	QHFSFPLDDR*	636.3	1006.5	21.8	y8	heavy
MYBBP1a	QHFSFPLDDR*	636.3	859.4	21.8	y7	heavy
MYBBP1a	QHFSFPLDDR*	636.3	625.3	21.8	y5	heavy
MYBBP1a	NAASQQDAVTEGAMPAATGK	959.5	1132.6	31.7	y12	light
MYBBP1a	NAASQQDAVTEGAMPAATGK	959.5	675.3	31.7	y7	light
MYBBP1a	NAASQQDAVTEGAMPAATGK	959.5	544.3	31.7	y6	light
MYBBP1a	NAASQQDAVTEGAMPAATGK	963.5	1140.6	31.7	y12	heavy
MYBBP1a	NAASQQDAVTEGAMPAATGK	963.5	683.4	31.7	y7	heavy
MYBBP1a	NAASQQDAVTEGAMPAATGK	963.5	552.3	31.7	y6	heavy
MYBBP1a	LSQVNGATPVSPIEPESK	927.0	1082.6	30.7	y10	light
MYBBP1a	LSQVNGATPVSPIEPESK	927.0	799.4	30.7	y7	light
MYBBP1a	LSQVNGATPVSPIEPESK	927.0	460.2	30.7	y4	light
MYBBP1a	LSQVNGATPVSPIEPESK	931.0	1090.6	30.7	y10	heavy
MYBBP1a	LSQVNGATPVSPIEPESK	931.0	807.4	30.7	y7	heavy
MYBBP1a	LSQVNGATPVSPIEPESK	931.0	468.3	30.7	y4	heavy

PPARG	LLAEISSDIDQLNPESADLR	1100.1	901.4	35.9	y8	light
PPARG	LLAEISSDIDQLNPESADLR	1100.1	787.4	35.9	y7	light
PPARG	LLAEISSDIDQLNPESADLR	1100.1	561.3	35.9	y5	light
PPARG	LLAEISSDIDQLNPESADLR	1105.1	911.4	35.9	y8	heavy
PPARG	LLAEISSDIDQLNPESADLR	1105.1	797.4	35.9	y7	heavy
PPARG	LLAEISSDIDQLNPESADLR	1105.1	571.3	35.9	y5	heavy
PPARG	SVEAVQEITEYAK*	733.9	1151.6	24.9	y10	light
PPARG	SVEAVQEITEYAK*	733.9	1080.6	24.9	y9	light
PPARG	SVEAVQEITEYAK*	733.9	981.5	24.9	y8	light
PPARG	SVEAVQEITEYAK*	733.9	853.4	24.9	y7	light
PPARG	SVEAVQEITEYAK*	733.9	724.4	24.9	y6	light
PPARG	SVEAVQEITEYAK*	733.9	611.3	24.9	y5	light
PPARG	SVEAVQEITEYAK*	733.9	510.3	24.9	y4	light
PPARG	SVEAVQEITEYAK*	737.9	1159.6	24.9	y10	heavy
PPARG	SVEAVQEITEYAK*	737.9	1088.6	24.9	y9	heavy
PPARG	SVEAVQEITEYAK*	738.9	989.5	24.9	y8	heavy
PPARG	SVEAVQEITEYAK*	737.9	861.4	24.9	y7	heavy
PPARG	SVEAVQEITEYAK*	737.9	732.4	24.9	y6	heavy
PPARG	SVEAVQEITEYAK*	737.9	619.3	24.9	y5	heavy
PPARG	SVEAVQEITEYAK*	737.9	518.3	24.9	y4	heavy
CEBPA	VLELTSDNDR*	581.3	820.4	20.3	y7	light
CEBPA	VLELTSDNDR*	581.3	707.3	20.3	y6	light
CEBPA	VLELTSDNDR*	581.3	606.2	20.3	y5	light
CEBPA	VLELTSDNDR*	586.3	830.4	20.3	y7	heavy
CEBPA	VLELTSDNDR*	586.3	717.3	20.3	y6	heavy
CEBPA	VLELTSDNDR*	586.3	616.3	20.3	y5	heavy
CEBPB	VLELTSDNDR	587.3	961.5	20.5	y8	light
CEBPB	VLELTSDNDR	587.3	832.4	20.5	y7	light
CEBPB	VLELTSDNDR	587.3	719.3	20.5	y6	light
CEBPB	VLELTSDNDR	592.3	971.5	20.5	y8	heavy
CEBPB	VLELTSDNDR	592.3	842.4	20.5	y7	heavy
CEBPB	VLELTSDNDR	592.3	729.3	20.5	y6	heavy
CEBPB	APAAEPAIGEHER*	674.3	1037.5	24	y9	light
CEBPB	APAAEPAIGEHER*	674.3	908.5	24	y8	light
CEBPB	APAAEPAIGEHER*	674.3	627.3	24	y5	light
CEBPB	APAAEPAIGEHER*	679.3	1047.5	24	y9	heavy
CEBPB	APAAEPAIGEHER*	679.3	918.5	24	y8	heavy
CEBPB	APAAEPAIGEHER*	679.3	637.3	24	y5	heavy
CEBPB	AAPAACFAGPPAAPAK	734.4	779.4	24.9	y9	light
CEBPB	AAPAACFAGPPAAPAK	734.4	708.4	24.9	y8	light
CEBPB	AAPAACFAGPPAAPAK	734.4	651.4	24.9	y7	light

CEBPB	AAPAACFAGPPAAPAK	738.4	787.5	24.9	y9	heavy
CEBPB	AAPAACFAGPPAAPAK	738.4	716.4	24.9	y8	heavy
CEBPB	AAPAACFAGPPAAPAK	738.4	659.4	24.9	y7	heavy
CEBPZ	MLSAILTGVNR*	587.8	930.5	20.5	y9	light
CEBPZ	MLSAILTGVNR*	587.8	659.4	20.5	y6	light
CEBPZ	MLSAILTGVNR*	587.8	546.3	20.5	y5	light
CEBPZ	MLSAILTGVNR*	592.8	940.5	20.5	y9	heavy
CEBPZ	MLSAILTGVNR*	592.8	669.4	20.5	y6	heavy
CEBPZ	MLSAILTGVNR*	592.8	556.3	20.5	y5	heavy
CEBPZ	ELLITDLLPDSR	692.9	916.5	21	y8	light
CEBPZ	ELLITDLLPDSR	692.9	587.3	21	y5	light
CEBPZ	ELLITDLLPDSR	692.9	474.2	21	y4	light
CEBPZ	ELLITDLLPDSR	697.9	926.5	21	y8	heavy
CEBPZ	ELLITDLLPDSR	697.9	597.3	21	y5	heavy
CEBPZ	ELLITDLLPDSR	697.9	484.2	21	y4	heavy
EEF1A1	IGGIGTVPVGR*	513.3	685.4	18.3	y7	light
EEF1A1	IGGIGTVPVGR*	513.3	628.4	18.3	y6	light
EEF1A1	IGGIGTVPVGR*	513.3	428.3	18.3	y4	light
EEF1A1	IGGIGTVPVGR*	518.3	695.4	18.3	y7	heavy
EEF1A1	IGGIGTVPVGR*	518.3	638.4	18.3	y6	heavy
EEF1A1	IGGIGTVPVGR*	518.3	438.3	18.3	y4	heavy
EEF1A1	YYVTIIDAPGHR	702.9	765.4	24	y7	light
EEF1A1	YYVTIIDAPGHR	702.9	652.3	24	y6	light
EEF1A1	YYVTIIDAPGHR	702.9	537.3	24	y5	light
EEF1A1	YYVTIIDAPGHR	707.9	775.4	24	y7	heavy
EEF1A1	YYVTIIDAPGHR	707.9	662.3	24	y6	heavy
EEF1A1	YYVTIIDAPGHR	707.9	547.3	24	y5	heavy
FLNA	SPFEVYVDK	542.3	752.4	19.2	y6	light
FLNA	SPFEVYVDK	542.3	623.3	19.2	y5	light
FLNA	SPFEVYVDK	542.3	524.3	19.2	y4	light
FLNA	SPFEVYVDK	546.3	760.4	19.2	y6	heavy
FLNA	SPFEVYVDK	546.3	631.4	19.2	y5	heavy
FLNA	SPFEVYVDK	546.3	532.3	19.2	y4	heavy
FLNA	YNDQHIPGSPFTAR*	801.9	832.4	27	y8	light
FLNA	YNDQHIPGSPFTAR*	801.9	735.4	27	y7	light
FLNA	YNDQHIPGSPFTAR*	801.9	591.3	27	y5	light
FLNA	YNDQHIPGSPFTAR*	806.9	842.4	27	y8	heavy
FLNA	YNDQHIPGSPFTAR*	806.9	745.4	27	y7	heavy
FLNA	YNDQHIPGSPFTAR*	806.9	601.3	27	y5	heavy
FOXC2	SEAASPALPVITK*	642.4	838.5	22.2	y8	light
FOXC2	SEAASPALPVITK*	642.4	670.4	22.2	y6	light

FOXC2	SEAASPALPVITK*	642.4	557.4	22.2	y5	light
FOXC2	SEAASPALPVITK*	646.4	846.6	22.2	y8	heavy
FOXC2	SEAASPALPVITK*	646.4	678.5	22.2	y6	heavy
FOXC2	SEAASPALPVITK*	646.4	565.4	22.2	y5	heavy
APEX1	EEAPDILCLQETK	773.4	891.5	26.1	y7	light
APEX1	EEAPDILCLQETK	773.4	778.4	26.1	y6	light
APEX1	EEAPDILCLQETK	773.4	618.3	26.1	y5	light
APEX1	EEAPDILCLQETK	777.4	899.5	26.1	y7	heavy
APEX1	EEAPDILCLQETK	777.4	786.4	26.1	y6	heavy
APEX1	EEAPDILCLQETK	777.4	626.4	26.1	y5	heavy
APEX1	ICSWNVDGLR*	610.3	946.5	21.2	y8	light
APEX1	ICSWNVDGLR*	610.3	859.4	21.2	y7	light
APEX1	ICSWNVDGLR*	610.3	673.4	21.2	y6	light
APEX1	ICSWNVDGLR*	615.3	956.5	21.2	y8	heavy
APEX1	ICSWNVDGLR*	615.3	869.5	21.2	y7	heavy
APEX1	ICSWNVDGLR*	615.3	683.4	21.2	y6	heavy
APEX1	VSYGIGEEEHDQEGR	568.9	870.4	23.9	y7	light
APEX1	VSYGIGEEEHDQEGR	568.9	741.3	23.9	y6	light
APEX1	VSYGIGEEEHDQEGR	568.9	604.3	23.9	y5	light
APEX1	VSYGIGEEEHDQEGR	572.3	880.4	23.9	y7	heavy
APEX1	VSYGIGEEEHDQEGR	572.3	751.3	23.9	y6	heavy
APEX1	VSYGIGEEEHDQEGR	572.3	614.3	23.9	y5	heavy
SMARCA5	TEQEEDEELLTESSK*	883.9	1150.5	29.4	y10	light
SMARCA5	TEQEEDEELLTESSK*	883.9	906.5	29.4	y8	light
SMARCA5	TEQEEDEELLTESSK*	883.9	777.4	29.4	y7	light
SMARCA5	TEQEEDEELLTESSK*	887.9	1158.6	29.4	y10	heavy
SMARCA5	TEQEEDEELLTESSK*	887.9	914.5	29.4	y8	heavy
SMARCA5	TEQEEDEELLTESSK*	887.9	785.4	29.4	y7	heavy
SMARCA5	ESEITDEDIDGILER	867.4	702.4	28.9	y6	light
SMARCA5	ESEITDEDIDGILER	867.4	587.4	28.9	y5	light
SMARCA5	ESEITDEDIDGILER	867.4	417.2	28.9	y3	light
SMARCA5	ESEITDEDIDGILER	872.4	712.4	28.9	y6	heavy
SMARCA5	ESEITDEDIDGILER	872.4	597.4	28.9	y5	heavy
SMARCA5	ESEITDEDIDGILER	872.4	427.3	28.9	y3	heavy
SMARCA4	GLQSYYAVAHAVTER	832.9	1116.6	27.9	y10	light
SMARCA4	GLQSYYAVAHAVTER	832.9	953.5	27.9	y9	light
SMARCA4	GLQSYYAVAHAVTER	832.9	783.4	27.9	y7	light
SMARCA4	GLQSYYAVAHAVTER	837.9	1126.6	27.9	y10	heavy
SMARCA4	GLQSYYAVAHAVTER	837.9	963.5	27.9	y9	heavy
SMARCA4	GLQSYYAVAHAVTER	837.9	793.4	27.9	y7	heavy
SMARCA4	GQPLPDHLQMAVQGK*	809.9	1223.6	27.2	y11	light

SMARCA4	GQPLPDHLQMAVQGK*	809.9	1011.5	27.2	y9	light
SMARCA4	GQPLPDHLQMAVQGK*	809.9	502.3	27.2	y5	light
SMARCA4	GQPLPDHLQMAVQGK*	813.9	1231.6	27.2	y11	heavy
SMARCA4	GQPLPDHLQMAVQGK*	813.9	1019.6	27.2	y9	heavy
SMARCA4	GQPLPDHLQMAVQGK*	813.9	510.3	27.2	y5	heavy
SMARC2D	AAFYHQPWAQEAVGR*	865.9	1141.6	28.9	y10	light
SMARC2D	AAFYHQPWAQEAVGR*	865.9	1013.5	28.9	y9	light
SMARC2D	AAFYHQPWAQEAVGR*	865.9	531.3	28.9	y5	light
SMARC2D	AAFYHQPWAQEAVGR*	870.9	1151.6	28.9	y10	heavy
SMARC2D	AAFYHQPWAQEAVGR*	870.9	1023.5	28.9	y9	heavy
SMARC2D	AAFYHQPWAQEAVGR*	870.9	541.3	28.9	y5	heavy
CSTF3	LVAQFPSSGR*	531.3	849.4	18.8	y8	light
CSTF3	LVAQFPSSGR*	531.3	650.3	18.8	y6	light
CSTF3	LVAQFPSSGR*	531.3	503.3	18.8	y5	light
CSTF3	LVAQFPSSGR*	536.3	859.4	18.8	y8	heavy
CSTF3	LVAQFPSSGR*	536.3	660.3	18.8	y6	heavy
CSTF3	LVAQFPSSGR*	536.3	513.3	18.8	y5	heavy
SFRS1	EAGDVCYADVYR*	709.3	946.4	24.2	y7	light
SFRS1	EAGDVCYADVYR*	709.3	786.4	24.2	y6	light
SFRS1	EAGDVCYADVYR*	709.3	623.3	24.2	y5	light
SFRS1	EAGDVCYADVYR*	714.3	956.4	24.2	y7	heavy
SFRS1	EAGDVCYADVYR*	714.3	796.4	24.2	y6	heavy
SFRS1	EAGDVCYADVYR*	714.3	633.3	24.2	y5	heavy
SFRS1	DGTGVVEFVR	539.8	805.5	19.1	y7	light
SFRS1	DGTGVVEFVR	539.8	649.4	19.1	y5	light
SFRS1	DGTGVVEFVR	539.8	550.3	19.1	y4	light
SFRS1	DGTGVVEFVR	544.8	815.5	19.1	y7	heavy
SFRS1	DGTGVVEFVR	544.8	659.4	19.1	y5	heavy
SFRS1	DGTGVVEFVR	544.8	560.3	19.1	y4	heavy
SFRS1	EDMTYAVR	492.7	740.4	17.7	y6	light
SFRS1	EDMTYAVR	492.7	609.3	17.7	y5	light
SFRS1	EDMTYAVR	492.7	508.3	17.7	y4	light
SFRS1	EDMTYAVR	497.7	750.4	17.7	y6	heavy
SFRS1	EDMTYAVR	497.7	619.3	17.7	y5	heavy
SFRS1	EDMTYAVR	497.7	518.3	17.7	y4	heavy
UBAP2L	LDFIGVEGSNYPR*	733.9	978.5	24.9	y9	light
UBAP2L	LDFIGVEGSNYPR*	733.9	822.4	24.9	y7	light
UBAP2L	LDFIGVEGSNYPR*	733.9	693.3	24.9	y6	light
UBAP2L	LDFIGVEGSNYPR*	738.9	988.5	24.9	y9	heavy
UBAP2L	LDFIGVEGSNYPR*	738.9	832.4	24.9	y7	heavy
UBAP2L	LDFIGVEGSNYPR*	738.9	703.3	24.9	y6	heavy

UBAP2L	DGSLASNPYSGDLTK	762.9	994.5	25.8	y9	light
UBAP2L	DGSLASNPYSGDLTK	762.9	880.4	25.8	y8	light
UBAP2L	DGSLASNPYSGDLTK	762.9	620.3	25.8	y6	light
UBAP2L	DGSLASNPYSGDLTK	766.9	1002.5	25.8	y9	heavy
UBAP2L	DGSLASNPYSGDLTK	766.9	888.5	25.8	y8	heavy
UBAP2L	DGSLASNPYSGDLTK	766.9	628.3	25.8	y6	heavy
NEDD4	LQNVAITGPAVPYSR	793.4	947.5	26.7	y9	light
NEDD4	LQNVAITGPAVPYSR	793.4	846.4	26.7	y8	light
NEDD4	LQNVAITGPAVPYSR	793.4	522.3	26.7	y4	light
NEDD4	LQNVAITGPAVPYSR	798.4	957.5	26.7	y9	heavy
NEDD4	LQNVAITGPAVPYSR	798.4	856.5	26.7	y8	heavy
NEDD4	LQNVAITGPAVPYSR	798.4	532.3	26.7	y4	heavy
NEDD4	TGGSEIVVTNK*	552.8	802.5	19.5	y7	light
NEDD4	TGGSEIVVTNK*	552.8	673.4	19.5	y6	light
NEDD4	TGGSEIVVTNK*	552.8	560.3	19.5	y5	light
NEDD4	TGGSEIVVTNK*	556.8	810.5	19.5	y7	heavy
NEDD4	TGGSEIVVTNK*	556.8	681.4	19.5	y6	heavy
NEDD4	TGGSEIVVTNK*	556.8	568.4	19.5	y5	heavy
CRRP1	TVYFAEEVQCEGNSFHK*	682.3	978.4	28.2	y8	light
CRRP1	TVYFAEEVQCEGNSFHK*	682.3	818.4	28.2	y7	light
CRRP1	TVYFAEEVQCEGNSFHK*	682.3	689.3	28.2	y6	light
CRRP1	TVYFAEEVQCEGNSFHK*	685.0	986.4	28.2	y8	heavy
CRRP1	TVYFAEEVQCEGNSFHK*	685.0	826.4	28.2	y7	heavy
CRRP1	TVYFAEEVQCEGNSFHK*	685.0	697.4	28.2	y6	heavy
NONO	FACHSASLTVR*	624.8	870.5	21.6	y8	light
NONO	FACHSASLTVR*	624.8	733.4	21.6	y7	light
NONO	FACHSASLTVR*	624.8	646.4	21.6	y6	light
NONO	FACHSASLTVR*	629.8	880.5	21.6	y8	heavy
NONO	FACHSASLTVR*	629.8	743.4	21.6	y7	heavy
NONO	FACHSASLTVR*	629.8	656.4	21.6	y6	heavy
MYH9	ALEQQVEEMK*	602.8	1020.5	21	y8	light
MYH9	ALEQQVEEMK*	602.8	635.3	21	y5	light
MYH9	ALEQQVEEMK*	602.8	536.2	21	y4	light
MYH9	ALEQQVEEMK*	606.8	1028.5	21	y8	heavy
MYH9	ALEQQVEEMK*	606.8	643.3	21	y5	heavy
MYH9	ALEQQVEEMK*	606.8	544.3	21	y4	heavy
ELAVL1	DANLYISGLPR	609.8	805.5	21.2	y7	light
ELAVL1	DANLYISGLPR	609.8	642.4	21.2	y6	light
ELAVL1	DANLYISGLPR	609.8	529.3	21.2	y5	light
ELAVL1	DANLYISGLPR	614.8	815.5	21.2	y7	heavy
ELAVL1	DANLYISGLPR	614.8	652.4	21.2	y6	heavy

ELAVL1	DANLYISGLPR	614.8	539.3	21.2	y5	heavy
ELAVL1	SLFSSIGEVESAK*	677.3	919.5	23.2	y9	light
ELAVL1	SLFSSIGEVESAK*	677.3	832.4	23.2	y8	light
ELAVL1	SLFSSIGEVESAK*	677.3	719.4	23.2	y7	light
ELAVL1	SLFSSIGEVESAK*	681.4	927.5	23.2	y9	heavy
ELAVL1	SLFSSIGEVESAK*	681.4	840.5	23.2	y8	heavy
ELAVL1	SLFSSIGEVESAK*	681.4	727.4	23.2	y7	heavy
GSK3B	LLEYTPTAR*	532.3	837.4	18.9	y7	light
GSK3B	LLEYTPTAR*	532.3	708.4	18.9	y6	light
GSK3B	LLEYTPTAR*	532.3	444.3	18.9	y4	light
GSK3B	LLEYTPTAR*	537.3	847.4	18.9	y7	heavy
GSK3B	LLEYTPTAR*	537.3	718.4	18.9	y6	heavy
GSK3B	LLEYTPTAR*	537.3	454.3	18.9	y4	heavy
GSK3B	TPPEAIALCSR	607.8	790.4	21.1	y7	light
GSK3B	TPPEAIALCSR	607.8	719.4	21.1	y6	light
GSK3B	TPPEAIALCSR	607.8	606.3	21.1	y5	light
GSK3B	TPPEAIALCSR	612.8	800.4	21.1	y7	heavy
GSK3B	TPPEAIALCSR	612.8	729.4	21.1	y6	heavy
GSK3B	TPPEAIALCSR	612.8	616.3	21.1	y5	heavy
LMNA C2	AAYEAELGDAR	583.3	731.4	20.4	y7	light
LMNA C2	AAYEAELGDAR	583.3	660.3	20.4	y6	light
LMNA C2	AAYEAELGDAR	583.3	418.2	20.4	y4	light
LMNA C2	AAYEAELGDAR	588.3	741.4	20.4	y7	heavy
LMNA C2	AAYEAELGDAR	588.3	670.3	20.4	y6	heavy
LMNA C2	AAYEAELGDAR	588.3	428.2	20.4	y4	heavy
LMNA C2	ITESEEVVSR	574.8	718.4	20.1	y6	light
LMNA C2	ITESEEVVSR	574.8	589.3	20.1	y5	light
LMNA C2	ITESEEVVSR	574.8	460.3	20.1	y4	light
LMNA C2	ITESEEVVSR	579.8	728.4	20.1	y6	heavy
LMNA C2	ITESEEVVSR	579.8	599.3	20.1	y5	heavy
LMNA C2	ITESEEVVSR	579.8	470.3	20.1	y4	heavy
LMNA C2	EGDLLAAQAR*	522.3	629.4	18.6	y6	light
LMNA C2	EGDLLAAQAR*	522.3	516.3	18.6	y5	light
LMNA C2	EGDLLAAQAR*	522.3	445.3	18.6	y4	light
LMNA C2	EGDLLAAQAR*	527.3	639.4	18.6	y6	heavy
LMNA C2	EGDLLAAQAR*	527.3	526.3	18.6	y5	heavy
LMNA C2	EGDLLAAQAR*	527.3	455.3	18.6	y4	heavy
NFKB1	VFETLEAR*	482.8	865.4	17.4	y7	light
NFKB1	VFETLEAR*	482.8	718.4	17.4	y6	light
NFKB1	VFETLEAR*	482.8	589.3	17.4	y5	light
NFKB1	VFETLEAR*	487.8	875.4	17.4	y7	heavy

NFKB1	VFETLEAR*	487.8	728.4	17.4	y6	heavy
NFKB1	VFETLEAR*	487.8	599.3	17.4	y5	heavy
NSUN2	IITVSMEDVK	567.8	708.3	19.9	y6	light
NSUN2	IITVSMEDVK	567.8	621.3	19.9	y5	light
NSUN2	IITVSMEDVK	567.8	490.3	19.9	y4	light
NSUN2	IITVSMEDVK	571.8	716.3	19.9	y6	heavy
NSUN2	IITVSMEDVK	571.8	629.3	19.9	y5	heavy
NSUN2	IITVSMEDVK	571.8	498.3	19.9	y4	heavy
NSUN2	LFEHYYQELK*	685.3	843.4	23.5	y6	light
NSUN2	LFEHYYQELK*	685.3	680.4	23.5	y5	light
NSUN2	LFEHYYQELK*	685.3	517.3	23.5	y4	light
NSUN2	LFEHYYQELK*	689.4	851.4	23.5	y6	heavy
NSUN2	LFEHYYQELK*	689.4	688.4	23.5	y5	heavy
NSUN2	LFEHYYQELK*	689.4	525.3	23.5	y4	heavy
NSUN2	TLLTQENPFFR	683.4	809.4	23.4	y6	light
NSUN2	TLLTQENPFFR	683.4	680.4	23.4	y5	light
NSUN2	TLLTQENPFFR	683.4	566.3	23.4	y4	light
NSUN2	TLLTQENPFFR	688.4	819.4	23.4	y6	heavy
NSUN2	TLLTQENPFFR	688.4	690.4	23.4	y5	heavy
NSUN2	TLLTQENPFFR	688.4	576.3	23.4	y4	heavy
PCBD2	NFNQAFGFMSR*	659.8	815.4	22.7	y7	light
PCBD2	NFNQAFGFMSR*	659.8	744.3	22.7	y6	light
PCBD2	NFNQAFGFMSR*	659.8	597.3	22.7	y5	light
PCBD2	NFNQAFGFMSR*	664.8	825.4	22.7	y7	heavy
PCBD2	NFNQAFGFMSR*	664.8	754.4	22.7	y6	heavy
PCBD2	NFNQAFGFMSR*	664.8	607.3	22.7	y5	heavy
RCOR1	VGPQYQAAVPDFDPAK*	851.9	1030.5	28.5	y10	light
RCOR1	VGPQYQAAVPDFDPAK*	851.9	888.4	28.5	y8	light
RCOR1	VGPQYQAAVPDFDPAK*	851.9	789.4	28.5	y7	light
RCOR1	VGPQYQAAVPDFDPAK*	855.9	1038.5	28.5	y10	heavy
RCOR1	VGPQYQAAVPDFDPAK*	855.9	896.5	28.5	y8	heavy
RCOR1	VGPQYQAAVPDFDPAK*	855.9	797.4	28.5	y7	heavy
SMARCC2	AGGSLCHILAAAYK*	716.4	1046.5	24.4	y9	light
SMARCC2	AGGSLCHILAAAYK*	716.4	886.5	24.4	y8	light
SMARCC2	AGGSLCHILAAAYK*	716.4	636.4	24.4	y6	light
SMARCC2	AGGSLCHILAAAYK*	716.4	523.3	24.4	y5	light
SMARCC2	AGGSLCHILAAAYK*	720.4	1054.6	24.4	y9	heavy
SMARCC2	AGGSLCHILAAAYK*	720.4	894.5	24.4	y8	heavy
SMARCC2	AGGSLCHILAAAYK*	720.4	644.4	24.4	y6	heavy
SMARCC2	AGGSLCHILAAAYK*	720.4	531.3	24.4	y5	heavy
SMARCC2	YIQAEPPTNK	580.8	685.4	20.3	y6	light

SMARCC2	YIQAEPPTNK	580.8	556.3	20.3	y5	light
SMARCC2	YIQAEPPTNK	580.8	459.3	20.3	y4	light
SMARCC2	YIQAEPPTNK	584.8	693.4	20.3	y6	heavy
SMARCC2	YIQAEPPTNK	584.8	564.3	20.3	y5	heavy
SMARCC2	YIQAEPPTNK	584.8	467.3	20.3	y4	heavy
TAX1BP3	VSEGGPAEIAGLQIGDK*	820.9	914.5	27.5	y9	light
TAX1BP3	VSEGGPAEIAGLQIGDK*	820.9	801.4	27.5	y8	light
TAX1BP3	VSEGGPAEIAGLQIGDK*	820.9	730.4	27.5	y7	light
TAX1BP3	VSEGGPAEIAGLQIGDK*	824.9	922.5	27.5	y9	heavy
TAX1BP3	VSEGGPAEIAGLQIGDK*	824.9	809.5	27.5	y8	heavy
TAX1BP3	VSEGGPAEIAGLQIGDK*	824.9	738.4	27.5	y7	heavy
TRIM28	LDLDLTSDSQPPVFK*	837.9	802.4	28	y7	light
TRIM28	LDLDLTSDSQPPVFK*	837.9	587.4	28	y5	light
TRIM28	LDLDLTSDSQPPVFK*	837.9	490.3	28	y4	light
TRIM28	LDLDLTSDSQPPVFK*	841.9	810.5	28	y7	heavy
TRIM28	LDLDLTSDSQPPVFK*	841.9	595.4	28	y5	heavy
TRIM28	LDLDLTSDSQPPVFK*	841.9	498.3	28	y4	heavy
TRIM28	SGEGEVSGLLR	552.3	644.4	19.5	y6	light
TRIM28	SGEGEVSGLLR	552.3	545.3	19.5	y5	light
TRIM28	SGEGEVSGLLR	552.3	458.3	19.5	y4	light
TRIM28	SGEGEVSGLLR	557.3	654.4	19.5	y6	heavy
TRIM28	SGEGEVSGLLR	557.3	555.3	19.5	y5	heavy
TRIM28	SGEGEVSGLLR	557.3	468.3	19.5	y4	heavy
TRIM28	DHQYQFLEDAVR	760.9	977.5	25.7	y8	light
TRIM28	DHQYQFLEDAVR	760.9	849.4	25.7	y7	light
TRIM28	DHQYQFLEDAVR	760.9	702.4	25.7	y6	light
TRIM28	DHQYQFLEDAVR	765.9	987.5	25.7	y8	heavy
TRIM28	DHQYQFLEDAVR	765.9	859.5	25.7	y7	heavy
TRIM28	DHQYQFLEDAVR	765.9	712.4	25.7	y6	heavy
ZFP326	ESVLTATSILNNPIVK	850.0	797.5	28.4	y7	light
ZFP326	ESVLTATSILNNPIVK	850.0	684.4	28.4	y6	light
ZFP326	ESVLTATSILNNPIVK	850.0	456.3	28.4	y4	light
ZFP326	ESVLTATSILNNPIVK	854.0	805.5	28.4	y7	heavy
ZFP326	ESVLTATSILNNPIVK	854.0	692.4	28.4	y6	heavy
ZFP326	ESVLTATSILNNPIVK	854.0	464.3	28.4	y4	heavy
ZFP326	NQGGSSWEAPYSR*	719.8	722.3	24.5	y6	light
ZFP326	NQGGSSWEAPYSR*	719.8	593.3	24.5	y5	light
ZFP326	NQGGSSWEAPYSR*	719.8	522.3	24.5	y4	light
ZFP326	NQGGSSWEAPYSR*	724.8	732.4	24.5	y6	heavy
ZFP326	NQGGSSWEAPYSR*	724.8	603.3	24.5	y5	heavy
ZFP326	NQGGSSWEAPYSR*	724.8	532.3	24.5	y4	heavy

AEBP1	TPSQEQLLAEALAAAR	834.9	772.4	28	y8	light
AEBP1	TPSQEQLLAEALAAAR	834.9	701.4	28	y7	light
AEBP1	TPSQEQLLAEALAAAR	840.0	782.4	28	y8	heavy
AEBP1	TPSQEQLLAEALAAAR	840.0	711.4	28	y7	heavy
AEBP1	YLSPDATVSTEVR*	719.4	791.4	24.5	y7	light
AEBP1	YLSPDATVSTEVR*	719.4	690.4	24.5	y6	light
AEBP1	YLSPDATVSTEVR*	719.4	591.3	24.5	y5	light
AEBP1	YLSPDATVSTEVR*	724.4	801.4	24.5	y7	heavy
AEBP1	YLSPDATVSTEVR*	724.4	700.4	24.5	y6	heavy
AEBP1	YLSPDATVSTEVR*	724.4	601.3	24.5	y5	heavy
AKAP8	GGISSGGEGVQDR	609.8	904.4	21.2	y9	light
AKAP8	GGISSGGEGVQDR	609.8	817.4	21.2	y8	light
AKAP8	GGISSGGEGVQDR	609.8	574.3	21.2	y5	light
AKAP8	GGISSGGEGVQDR	614.8	914.4	21.2	y9	heavy
AKAP8	GGISSGGEGVQDR	614.8	827.4	21.2	y8	heavy
AKAP8	GGISSGGEGVQDR	614.8	584.3	21.2	y5	heavy
AKAP8	LLEEQTCEAASETR*	818.9	1024.4	27.5	y9	light
AKAP8	LLEEQTCEAASETR*	818.9	563.3	27.5	y5	light
AKAP8	LLEEQTCEAASETR*	818.9	492.2	27.5	y4	light
AKAP8	LLEEQTCEAASETR*	823.9	1034.4	27.5	y9	heavy
AKAP8	LLEEQTCEAASETR*	823.9	573.3	27.5	y5	heavy
AKAP8	LLEEQTCEAASETR*	823.9	502.2	27.5	y4	heavy
CTNNB1	MMVCQVGGIEALVR	781.9	913.5	26.4	y9	light
CTNNB1	MMVCQVGGIEALVR	781.9	814.5	26.4	y8	light
CTNNB1	MMVCQVGGIEALVR	781.9	757.5	26.4	y7	light
CTNNB1	MMVCQVGGIEALVR	786.9	923.6	26.4	y9	heavy
CTNNB1	MMVCQVGGIEALVR	786.9	824.5	26.4	y8	heavy
CTNNB1	MMVCQVGGIEALVR	786.9	767.5	26.4	y7	heavy
CTNNB1	QDVYGPQPQVR	643.8	781.4	22.2	y7	light
CTNNB1	QDVYGPQPQVR	643.8	724.4	22.2	y6	light
CTNNB1	QDVYGPQPQVR	643.8	499.3	22.2	y4	light
CTNNB1	QDVYGPQPQVR	648.8	791.4	22.2	y7	heavy
CTNNB1	QDVYGPQPQVR	648.8	734.4	22.2	y6	heavy
CTNNB1	QDVYGPQPQVR	648.8	509.3	22.2	y4	heavy
CTNNB1	SDFQVNLNNASR	682.8	887.5	23.4	y8	light
CTNNB1	SDFQVNLNNASR	682.8	788.4	23.4	y7	light
CTNNB1	SDFQVNLNNASR	682.8	561.3	23.4	y5	light
CTNNB1	SDFQVNLNNASR	687.8	897.5	23.4	y8	heavy
CTNNB1	SDFQVNLNNASR	687.8	798.4	23.4	y7	heavy
CTNNB1	SDFQVNLNNASR	687.8	571.3	23.4	y5	heavy
EMERIN	IFEYETQR	543.3	972.4	19.2	y7	light

EMERIN	IFEYETQR	543.3	825.4	19.2	y6	light
EMERIN	IFEYETQR	543.3	696.3	19.2	y5	light
EMERIN	IFEYETQR	548.3	982.5	19.2	y7	heavy
EMERIN	IFEYETQR	548.3	835.4	19.2	y6	heavy
EMERIN	IFEYETQR	548.3	706.3	19.2	y5	heavy
EMERIN	TYGEPESVGMSK*	642.8	834.4	22.2	y8	light
EMERIN	TYGEPESVGMSK*	642.8	608.3	22.2	y6	light
EMERIN	TYGEPESVGMSK*	642.8	422.2	22.2	y4	light
EMERIN	TYGEPESVGMSK*	646.8	842.4	22.2	y8	heavy
EMERIN	TYGEPESVGMSK*	646.8	616.3	22.2	y6	heavy
EMERIN	TYGEPESVGMSK*	646.8	430.2	22.2	y4	heavy
RAD50	ILELDQELTK	601.3	733.4	20.9	y6	light
RAD50	ILELDQELTK	601.3	618.3	20.9	y5	light
RAD50	ILELDQELTK	601.3	490.3	20.9	y4	light
RAD50	ILELDQELTK	605.3	741.4	20.9	y6	heavy
RAD50	ILELDQELTK	605.3	626.4	20.9	y5	heavy
RAD50	ILELDQELTK	605.3	498.3	20.9	y4	heavy
RAD50	LIQDQQEQIQHLK	810.9	895.5	27.2	y7	light
RAD50	LIQDQQEQIQHLK	810.9	638.4	27.2	y5	light
RAD50	LIQDQQEQIQHLK	810.9	525.3	27.2	y4	light
RAD50	LIQDQQEQIQHLK	814.9	903.5	27.2	y7	heavy
RAD50	LIQDQQEQIQHLK	814.9	646.4	27.2	y5	heavy
RAD50	LIQDQQEQIQHLK	814.9	533.3	27.2	y4	heavy
RAD50	SELQQLEGSSDR*	674.8	763.4	23.1	y7	light
RAD50	SELQQLEGSSDR*	674.8	650.3	23.1	y6	light
RAD50	SELQQLEGSSDR*	674.8	521.2	23.1	y5	light
RAD50	SELQQLEGSSDR*	679.8	773.4	23.1	y7	heavy
RAD50	SELQQLEGSSDR*	679.8	660.3	23.1	y6	heavy
RAD50	SELQQLEGSSDR*	679.8	531.2	23.1	y5	heavy
RAD50	VCLTDVTIMER	668.8	863.4	23	y7	light
RAD50	VCLTDVTIMER	668.8	748.4	23	y6	light
RAD50	VCLTDVTIMER	668.8	649.3	23	y5	light
RAD50	VCLTDVTIMER	673.8	873.4	23	y7	heavy
RAD50	VCLTDVTIMER	673.8	758.4	23	y6	heavy
RAD50	VCLTDVTIMER	673.8	659.3	23	y5	heavy
RUNX2	GTGLPAITDVPR*	598.8	700.4	20.9	y6	light
RUNX2	GTGLPAITDVPR*	598.8	771.4	20.9	y7	light
RUNX2	GTGLPAITDVPR*	598.8	868.5	20.9	y8	light
RUNX2	GTGLPAITDVPR*	598.8	710.4	20.9	y6	heavy
RUNX2	GTGLPAITDVPR*	598.8	781.4	20.9	y7	heavy
RUNX2	GTGLPAITDVPR*	603.8	878.5	20.9	y8	heavy

RUVBL1	AVLLAGPPGTGK	540.8	684.4	19.1	y8	light
RUVBL1	AVLLAGPPGTGK	540.8	613.3	19.1	y7	light
RUVBL1	AVLLAGPPGTGK	540.8	556.3	19.1	y6	light
RUVBL1	AVLLAGPPGTGK	544.8	692.4	19.1	y8	heavy
RUVBL1	AVLLAGPPGTGK	544.8	621.3	19.1	y7	heavy
RUVBL1	AVLLAGPPGTGK	544.8	564.3	19.1	y6	heavy
RUVBL1	EACGVIVELIK	615.8	714.5	21.4	y6	light
RUVBL1	EACGVIVELIK	615.8	601.4	21.4	y5	light
RUVBL1	EACGVIVELIK	615.8	502.3	21.4	y4	light
RUVBL1	EACGVIVELIK	619.8	722.5	21.4	y6	heavy
RUVBL1	EACGVIVELIK	619.8	609.4	21.4	y5	heavy
RUVBL1	EACGVIVELIK	619.8	510.3	21.4	y4	heavy
RUVBL1	QAASGLVGQENAR*	650.8	943.5	22.4	y9	light
RUVBL1	QAASGLVGQENAR*	650.8	773.4	22.4	y7	light
RUVBL1	QAASGLVGQENAR*	650.8	674.3	22.4	y6	light
RUVBL1	QAASGLVGQENAR*	655.8	953.5	22.4	y9	heavy
RUVBL1	QAASGLVGQENAR*	655.8	783.4	22.4	y7	heavy
RUVBL1	QAASGLVGQENAR*	655.8	684.3	22.4	y6	heavy
RUVBL1	TALALAIAQELGSK	693.4	916.5	23.7	y9	light
RUVBL1	TALALAIAQELGSK	693.4	845.5	23.7	y8	light
RUVBL1	TALALAIAQELGSK	693.4	732.4	23.7	y7	light
RUVBL1	TALALAIAQELGSK	697.4	924.5	23.7	y9	heavy
RUVBL1	TALALAIAQELGSK	697.4	853.5	23.7	y8	heavy
RUVBL1	TALALAIAQELGSK	697.4	740.4	23.7	y7	heavy
RUVBL1	VPFCPMVGSEVYSTEIK	972.0	1439.7	32.1	y13	light
RUVBL1	VPFCPMVGSEVYSTEIK	972.0	1112.5	32.1	y10	light
RUVBL1	VPFCPMVGSEVYSTEIK	972.0	577.3	32.1	y5	light
RUVBL1	VPFCPMVGSEVYSTEIK	976.0	1447.7	32.1	y13	heavy
RUVBL1	VPFCPMVGSEVYSTEIK	976.0	1120.6	32.1	y10	heavy
RUVBL1	VPFCPMVGSEVYSTEIK	976.0	585.3	32.1	y5	heavy
LPIN1	GHNTGEQPAQLGLATR*	825.4	926.5	27.7	y9	light
LPIN1	GHNTGEQPAQLGLATR*	825.4	630.4	27.7	y6	light
LPIN1	GHNTGEQPAQLGLATR*	825.4	517.3	27.7	y5	light
LPIN1	GHNTGEQPAQLGLATR*	830.4	936.6	27.7	y9	heavy
LPIN1	GHNTGEQPAQLGLATR*	830.4	640.4	27.7	y6	heavy
LPIN1	GHNTGEQPAQLGLATR*	830.4	527.3	27.7	y5	heavy
RUVBL2	LLIVSTSPYSEK	668.9	898.4	23	y8	light
RUVBL2	LLIVSTSPYSEK	668.9	811.4	23	y7	light
RUVBL2	LLIVSTSPYSEK	668.9	623.3	23	y5	light
RUVBL2	LLIVSTSPYSEK	672.9	906.4	23	y8	heavy
RUVBL2	LLIVSTSPYSEK	672.9	819.4	23	y7	heavy

RUVBL2	LLIVSTSPYSEK	672.9	631.3	23	y5	heavy
RUVBL2	TQGFLALFSGDTGEIK	842.4	1137.6	28.2	y11	light
RUVBL2	TQGFLALFSGDTGEIK	842.4	953.5	28.2	y9	light
RUVBL2	TQGFLALFSGDTGEIK	842.4	806.4	28.2	y8	light
RUVBL2	TQGFLALFSGDTGEIK	846.4	1145.6	28.2	y11	heavy
RUVBL2	TQGFLALFSGDTGEIK	846.4	961.5	28.2	y9	heavy
RUVBL2	TQGFLALFSGDTGEIK	846.4	814.4	28.2	y8	heavy
RUVBL2	VYSLFLDESR*	614.8	766.4	21.3	y6	light
RUVBL2	VYSLFLDESR*	614.8	619.3	21.3	y5	light
RUVBL2	VYSLFLDESR*	614.8	506.2	21.3	y4	light
RUVBL2	VYSLFLDESR*	619.8	776.4	21.3	y6	heavy
RUVBL2	VYSLFLDESR*	619.8	629.3	21.3	y5	heavy
RUVBL2	VYSLFLDESR*	619.8	516.2	21.3	y4	heavy
WDR5	YILAATLDNTLK	668.4	875.5	23	y8	light
WDR5	YILAATLDNTLK	668.4	804.4	23	y7	light
WDR5	YILAATLDNTLK	668.4	703.4	23	y6	light
WDR5	YILAATLDNTLK	672.4	883.5	23	y8	heavy
WDR5	YILAATLDNTLK	672.4	812.5	23	y7	heavy
WDR5	YILAATLDNTLK	672.4	711.4	23	y6	heavy
WDR5	TLIDDDNPPVSFVK*	780.4	887.5	26.3	y8	light
WDR5	TLIDDDNPPVSFVK*	780.4	773.5	26.3	y7	light
WDR5	TLIDDDNPPVSFVK*	780.4	480.3	26.3	y4	light
WDR5	TLIDDDNPPVSFVK*	784.4	895.5	26.3	y8	heavy
WDR5	TLIDDDNPPVSFVK*	784.4	781.5	26.3	y7	heavy
WDR5	TLIDDDNPPVSFVK*	784.4	488.3	26.3	y4	heavy
NFIL3	FIATQPISASDSR	696.9	960.5	23.8	y9	light
NFIL3	FIATQPISASDSR	696.9	832.4	23.8	y8	light
NFIL3	FIATQPISASDSR	696.9	735.4	23.8	y7	light
NFIL3	FIATQPISASDSR	701.9	970.5	23.8	y9	heavy
NFIL3	FIATQPISASDSR	701.9	842.4	23.8	y8	heavy
NFIL3	FIATQPISASDSR	701.9	745.4	23.8	y7	heavy
NFIL3	LIALGEENATLK	636.4	974.5	22	y9	light
NFIL3	LIALGEENATLK	636.4	861.4	22	y8	light
NFIL3	LIALGEENATLK	636.4	804.4	22	y7	light
NFIL3	LIALGEENATLK	640.4	982.5	22	y9	heavy
NFIL3	LIALGEENATLK	640.4	869.4	22	y8	heavy
NFIL3	LIALGEENATLK	640.4	812.4	22	y7	heavy
NFIL3	QEPVELESFAR*	652.8	1047.5	22.5	y9	light
NFIL3	QEPVELESFAR*	652.8	851.4	22.5	y7	light
NFIL3	QEPVELESFAR*	652.8	722.4	22.5	y6	light
NFIL3	QEPVELESFAR*	657.8	1057.6	22.5	y9	heavy

NFIL3	QEPVELESFAR*	657.8	861.4	22.5	y7	heavy
NFIL3	QEPVELESFAR*	657.8	732.4	22.5	y6	heavy
FOXK1	TPFGPLSSR*	481.3	763.4	17.3	y7	light
FOXK1	TPFGPLSSR*	481.3	616.3	17.3	y6	light
FOXK1	TPFGPLSSR*	481.3	559.3	17.3	y5	light
FOXK1	TPFGPLSSR*	486.3	773.4	17.3	y7	heavy
FOXK1	TPFGPLSSR*	486.3	626.3	17.3	y6	heavy
FOXK1	TPFGPLSSR*	486.3	569.3	17.3	y5	heavy
SIRT2	NLFTQTLGLGSQK*	703.9	589.3	24	y6	light
SIRT2	NLFTQTLGLGSQK*	703.9	532.3	24	y5	light
SIRT2	NLFTQTLGLGSQK*	707.9	597.3	24	y6	heavy
SIRT2	NLFTQTLGLGSQK*	707.9	540.3	24	y5	heavy
BRD8	SSAAGDIGEADGSSGK*	704.8	1092.5	24	y12	light
BRD8	SSAAGDIGEADGSSGK*	704.8	621.3	24	y7	light
BRD8	SSAAGDIGEADGSSGK*	704.8	435.2	24	y5	light
BRD8	SSAAGDIGEADGSSGK*	708.8	1100.5	24	y12	heavy
BRD8	SSAAGDIGEADGSSGK*	708.8	629.3	24	y7	heavy
BRD8	SSAAGDIGEADGSSGK*	708.8	443.2	24	y5	heavy
FABP4	EVGVGFATR	468.3	707.4	17	y7	light
FABP4	EVGVGFATR	468.3	551.3	17	y5	light
FABP4	EVGVGFATR	468.3	494.3	17	y4	light
FABP4	EVGVGFATR	473.3	717.4	17	y7	heavy
FABP4	EVGVGFATR	473.3	561.3	17	y5	heavy
FABP4	EVGVGFATR	473.3	504.3	17	y4	heavy
FABP4	LVSSENFDDYMK*	724.3	932.4	24.6	y7	light
FABP4	LVSSENFDDYMK*	724.3	818.3	24.6	y6	light
FABP4	LVSSENFDDYMK*	724.3	671.3	24.6	y5	light
FABP4	LVSSENFDDYMK*	728.3	940.4	24.6	y7	heavy
FABP4	LVSSENFDDYMK*	728.3	826.4	24.6	y6	heavy
FABP4	LVSSENFDDYMK*	728.3	679.3	24.6	y5	heavy
SMARCC1	TLAGLVVQLLQFQEDAFGK*	693.0	941.4	28.6	y8	light
SMARCC1	TLAGLVVQLLQFQEDAFGK*	693.0	794.4	28.6	y7	light
SMARCC1	TLAGLVVQLLQFQEDAFGK*	693.0	537.3	28.6	y5	light
SMARCC1	TLAGLVVQLLQFQEDAFGK*	695.7	949.5	28.6	y8	heavy
SMARCC1	TLAGLVVQLLQFQEDAFGK*	695.7	802.4	28.6	y7	heavy
SMARCC1	TLAGLVVQLLQFQEDAFGK*	695.7	545.3	28.6	y5	heavy
SF3B3	LGAVFNQVAFPLQYTPR*	961.0	1092.6	31.7	y9	light
SF3B3	LGAVFNQVAFPLQYTPR*	961.0	1021.5	31.7	y8	light
SF3B3	LGAVFNQVAFPLQYTPR*	961.0	874.5	31.7	y7	light
SF3B3	LGAVFNQVAFPLQYTPR*	966.0	1102.6	31.7	y9	heavy
SF3B3	LGAVFNQVAFPLQYTPR*	966.0	1031.6	31.7	y8	heavy

SF3B3	LGAVFNQVAFPLQYTPR*	966.0	884.5	31.7	y7	heavy
SF3B3	AVMISAIEK	481.3	791.4	17.3	y7	light
SF3B3	AVMISAIEK	481.3	660.4	17.3	y6	light
SF3B3	AVMISAIEK	481.3	547.3	17.3	y5	light
SF3B3	AVMISAIEK	485.3	799.4	17.3	y7	heavy
SF3B3	AVMISAIEK	485.3	668.4	17.3	y6	heavy
SF3B3	AVMISAIEK	485.3	555.3	17.3	y5	heavy
SF3B3	DYIVVGSDSGR*	584.3	677.3	20.4	y7	light
SF3B3	DYIVVGSDSGR*	584.3	578.3	20.4	y6	light
SF3B3	DYIVVGSDSGR*	589.3	687.3	20.4	y7	heavy
SF3B3	DYIVVGSDSGR*	589.3	588.3	20.4	y6	heavy
HNRNPA2B1	GFGFVTFDDHDPVDK	565.9	825.4	23.8	y7	light
HNRNPA2B1	GFGFVTFDDHDPVDK	565.9	458.3	23.8	y4	light
HNRNPA2B1	GFGFVTFDDHDPVDK	568.6	833.4	23.8	y7	heavy
HNRNPA2B1	GFGFVTFDDHDPVDK	568.6	466.3	23.8	y4	heavy
HNRNPA2B1	GGNFGFGDSR*	507.2	638.3	18.1	y6	light
HNRNPA2B1	GGNFGFGDSR*	507.2	581.3	18.1	y5	light
HNRNPA2B1	GGNFGFGDSR*	512.2	648.3	18.1	y6	heavy
HNRNPA2B1	GGNFGFGDSR*	512.2	591.3	18.1	y5	heavy
HNRNPA2B1	GGGGNFGPGPGSNFR	689.3	888.4	23.6	y9	light
HNRNPA2B1	GGGGNFGPGPGSNFR	689.3	831.4	23.6	y8	light
HNRNPA2B1	GGGGNFGPGPGSNFR	694.3	898.4	23.6	y9	heavy
HNRNPA2B1	GGGGNFGPGPGSNFR	694.3	841.4	23.6	y8	heavy
HNRNPAB	IFVGGLNPEATEEK*	752.4	917.4	25.5	y8	light
HNRNPAB	IFVGGLNPEATEEK*	752.4	803.4	25.5	y7	light
HNRNPAB	IFVGGLNPEATEEK*	756.4	925.4	25.5	y8	heavy
HNRNPAB	IFVGGLNPEATEEK*	756.4	811.4	25.5	y7	heavy
HNRNPAB	EVYQQQQYGSGGR	750.3	980.5	25.4	y9	light
HNRNPAB	EVYQQQQYGSGGR	750.3	852.4	25.4	y8	light
HNRNPAB	EVYQQQQYGSGGR	755.4	990.5	25.4	y9	heavy
HNRNPAB	EVYQQQQYGSGGR	755.4	862.4	25.4	y8	heavy

Table S3: Primers used to make siRNA

	Gene	NP number	First primer Forward	First primer Backward	Nested primer Forward	Nested primer Backward
1	Pparg	NP_035276	tccgaatttttcaagggtgcc	caagtccttgtagatctcctg	gcgtaatacgactcactatagggtttcgatccgtagaagcc	gcgtaatacgactcactatagggtgaaggctcatgtctgtc
2	C/ebpa	NP_031704	cccacttgcagttccagatc	gaaaccatcctctgggtctc	gcgtaatacgactcactataggagaccaccatgcacctac	gcgtaatacgactcactataggcaaggcggtcccgcag
3	C/EBPβ	NP_034013	actacggttacgtgagcctc	ggcagctgcttgaacaagttc	gcgtaatacgactcactatagggccgcccgcctgcttc	gcgtaatacgactcactataggagctgctccaccttcttc
4	C/ebpz 1	NP_001019977	aagacgacaactgcttcccac	ttcctctgccgtttgggtttc	gcgtaatacgactcactatagggccagcaatatgaaaaaagc	gcgtaatacgactcactatagggggggctttcatcttcttcc
	C/ebpz 2	NP_001019977	cagaagatccggatgaggaa	ccagggctttgtacttggac	gcgtaatacgactcactatagggcgatgagggcaagaatg	gcgtaatacgactcactataggcttggacacgacatctggag
5	Fabp4 1	NP_077717	gtgtgatgcctttgtgggaac	aaactcttgtggaagtcacgc	gcgtaatacgactcactataggtggaagcttgtctccagtg	gcgtaatacgactcactataggaacacattccaccaccagc
	Fabp4 2	NP_077717	ccgagatttccttcaaactgg	ccatatccaataaaatgcatcttc	gcgtaatacgactcactataggcgatgaaatcaccgcagac	gcgtaatacgactcactataggtaattgcttgcttattagtgg
6	Foxk1	NP_951031	aacgggtacatcctggctag	tgccatagctgtgggctgtg	gcgtaatacgactcactataggacgacacagcaggcacag	gcgtaatacgactcactataggtctacccgggacctcttg
7	Mybbp1a	NP_058056	gccaaggatattcctagtgac	ctggccactctcctttcttg	gcgtaatacgactcactataggcaaagcggaagaaaaaggg	gcgtaatacgactcactataggaccccactctgtaacagg
8	Sirt2	NP_001116238	cacatcacactgtgtcaacac	gctgttcctctttctctttgg	gcgtaatacgactcactataggagaatacacgatgggctgg	gcgtaatacgactcactataggggactttccaggggagatg
9	Csrp1	NP_031817	aggcaagaaatgtggggtatg	tcactctgagtgaaccaaggc	gcgtaatacgactcactatagggacggtctactttgctgag	gcgtaatacgactcactataggccctgtccaaagccaaaac
10	Brd8	NP_084423	agttttccgtgtgcagtgaag	tatctgcttcaatggcacagc	gcgtaatacgactcactataggcaagaagcaattcaggctc	gcgtaatacgactcactataggtggttccccctcaaagag
11	Wdr5	NP_543124	aacttcaaccccccagtccaac	ttagcagtcacttcttccacag	gcgtaatacgactcactataggagtgtgaggatatgggacg	gcgtaatacgactcactataggtgtcgttctctaacgctgc
12	Eef1a1	NP_034236	gtggagactggtgttctcaag	ttagccttctgagctttctgg	gcgtaatacgactcactatagggggcatggtggttaccttg	Gcgtaatacgactcactatagggcagacttggtgactttgc

13	Flna 1	NP_034357	tgtgaacacaag caatgcagg	agggtaccata atgcggtatg	gcgtaatacgactcact atagggccctttcggtta ccattg	gcgtaatacgactcac tataggtgcctgggat atgctcatc
	Flna 2	NP_034357	ggcagtccctttt ctgtgaa	tgtgctcctcgt tgaacttg	gcgtaatacgactcact ataggggccgggtgaa agagagtat	gcgtaatacgactcac tataggtgtgctcctcg ttgaacttg
	Flna 3	NP_034357	gagctgacaaca gcgtggta	aggtaatggtg tgtgtgcca	gcgtaatacgactcact ataggtgtacctggcag tccctttc	gcgtaatacgactcac tataggaggtaatggt gtgtgtgcca
14	Foxc2	NP_038547	accgctggcact gccatac	ttggtgcagtcg taagagtag	gcgtaatacgactcact atagggcttacacgcag ccgtg	gcgtaatacgactcac tatagggacggcgtag ctcgatag
15	Apex1	NP_033817	cagctccgtcag acaaagaag	cacagtgctag gtaaagggtg	gcgtaatacgactcact ataggtggtgtgggcct actttc	gcgtaatacgactcac tataggatgggacagt ggtcactg
16	Smarca5	NP_444354	tcaaggctaatg agaagtggg	gcttctttttttct tccacggc	gcgtaatacgactcact ataggtagccagagaa gtagaagg	gcgtaatacgactcac tataggaccgtccatct tacgtttc
17	Smarca4	NP_001122316	agaaactctccc ctaacccac	agtcttcttcgc tgccacttc	gcgtaatacgactcact atagggaagattgtgga tgccgtg	gcgtaatacgactcac tataggtcctcttgttcc tcctcac
18	Smarcd2	NP_001123659	caggcactgtgg ctttacatc	ttaggtcaggc gaattcccag	gcgtaatacgactcact ataggaaacacaacca gctgcagg	gcgtaatacgactcac tataggtgttccagttc ctgccttc
19	Smarcc1	NP_033237	cgacattttgaag agctggag	accccatctgc aggaggag	gcgtaatacgactcact ataggtggacagagag aaagaggc	gcgtaatacgactcac tataggtggtggagga ggatacatg
20	Smarcc2	NP_937803	aactccgacattt tgaggagc	tcactgtggag gtggcacag	gcgtaatacgactcact ataggggagacaataat ggaccgg	gcgtaatacgactcac tataggtgactgtgcct gggcttg
21	Cstf3	NP_663504	aggaaacagctt tactggtgg	tcatcgtattcg cttctgctg	gcgtaatacgactcact ataggtacccttgttctg caagtg	gcgtaatacgactcac tataggaatgtcatga acaggggg
22	Sf3b3	NP_598714	ctttgctgatgac acctatcc	aaggcatagcg ggtcctaatg	gcgtaatacgactcact ataggcagccttctcga ctatgac	gcgtaatacgactcac tataggcctcaagcttc ttggacac
23	Hnrnpa2b1	NP_872591	aggaagatactg aggaacacc	tatctgctccttc caccatag	gcgtaatacgactcact ataggaccttagagatt actttgaag	gcgtaatacgactcac tataggacttcctccag gaccatag
24	Sfrs1	NP_001071635	aacaacgactgc cgcatctac	gtgtataacctа cctcgtgag	gcgtaatacgactcact ataggaacctacctccg gatatcc	gcgtaatacgactcac tataggccagttttcga actgcatac
25	Hnrnpab	NP_034578	gtttggagaggtt gttgactg	gttattctgatg accaccacg	gcgtaatacgactcact ataggatggatcccaac actggac	gcgtaatacgactcac tataggttgtactaccc tgacctcc
26	Polr2h	NP_663607	tcgatgtgaaag acatcgacc	cagaaggccag cttcttcatc	gcgtaatacgactcact ataggatttgaccgagt	gcgtaatacgactcac tataggaaactctgga

					atcccgg	gtccacctc
27	Ubap2l	NP_082751	acgcagcagacattcctgaac	tattcaccaagctggtcatcg	gcgtaatacgactcactatagggcctcctggctatagttac	gcgtaatacgactcactataggcgagagtgaggatatcctg
28	Nedd4	NP_035020	tttggacagacacatcagcac	ctaatcaacgccatcaaagcc	gcgtaatacgactcactataggctgaaaaccggaggatcag	gcgtaatacgactcactataggctgtgtgttctcaattgcc
29	Ptbp1	NP_032982	gctgggaattctgtccttttg	agatggtggacttggaaaagg	gcgtaatacgactcactatagggtcagcaatctgaaccctg	gcgtaatacgactcactataggggtcatggttgtgcagttc
30	Nono	NP_075633	gcactcattgagatggagaag	atatcggcggcgtttatttgg	gcgtaatacgactcactataggcaacagcaggatcaagtgg	gcgtaatacgactcactataggtgaatgcaggaggagttcc
31	Nfil3	NP_059069	cactagcaactccccaagaac	gagatcggttgtgtggctatg	gcgtaatacgactcactatagggtgtagtgggcaagtcttc	gcgtaatacgactcactataggatctcttgagcgagaccac
32	Creb1	NP_034082	gggtgccaaggattgaagaag	gatttgtggcagtaaaggtcc	gcgtaatacgactcactataggcagaagaggagacttcagc	gcgtaatacgactcactatagggtgcttttagctcctcaatc
33	Smarce1	NP_065643	gtcggttgtcacaacagctag	actccttcttctcgtcttctg	gcgtaatacgactcactataggcaggtccagtcttttaatgg	gcgtaatacgactcactataggtccactgtggcgctgttg
34	Mgmt	NP_032624	tttggggaagatggagctgtc	gtcgactcgaaggatgacttg	gcgtaatacgactcactataggatgggatacggttgctcag	gcgtaatacgactcactatagggtcccagtcagacccaag
35	Trim28	NP_035718	gacctggtcatgtgtaaccag	agagagctcctgagaacttag	gcgtaatacgactcactataggttgcttccacctggattgc	gcgtaatacgactcactatagggcactgggaaggttcaatg
36	Myh9	NP_071855	ataaacaccgacctgaacctg	ctattcagctgccttggcatc	gcgtaatacgactcactataggagccacgcacagaagaatg	gcgtaatacgactcactataggcatctgcttttaccgtcgac
37	Lpin1	NP_001123884	attttgcccacgctgggaaag	caagctgaggctgaatgcatg	gcgtaatacgactcactataggtcaccagggcattgcaaag	gcgtaatacgactcactataggttcaaaaggtggcagtggc
38	Runx2	NP_001139510	tgcccaggcgtattcagatg	caatatggccgccaaacagac	gcgtaatacgactcactataggatgacactgccacctctg	gcgtaatacgactcactataggtcatccattctgccgctag
39	GL3	NP_680372			gcgtaatacgactcactatagggcggtcggtaaagttgttc	gcgtaatacgactcactataggtcttgcgtcgagttttccg
40	Lac1	NP_012917			gcgtaatacgactcactataggcggcgatggcggagctgaat	gcgtaatacgactcactatagggcagacgcgccgagacagaa
41	Gus1	NP_200933			gcgtaatacgactcactataggcgtcctgtagaaaccccaacccg	gcgtaatacgactcactataggCCCGGCGGGATAGTCTGCCA

42	YFP				gcgtaatacgactcactataggcatcctggtcgagctggac	gcgtaatacgactcactataggcgttggggtcttgctcag

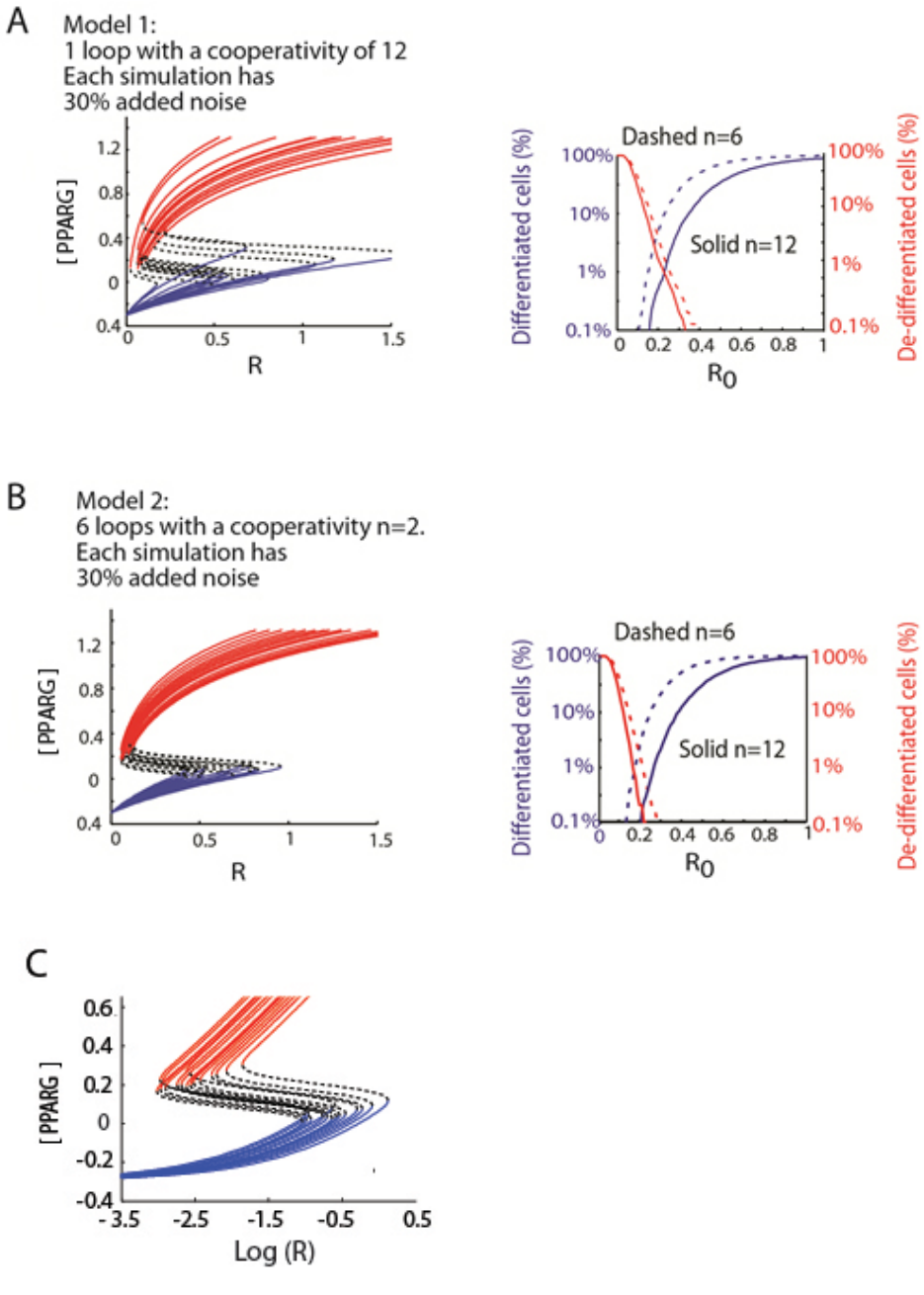

Figure S1. Identifying the system architecture needed to both control low rates of differentiation and to prevent dedifferentiation. (A) Increased cooperativity significantly increases the parameter variation and the ability to have graded control over small rates of differentiation. However, a single loop system (Model 1 from Fig. 2) even if it has a cooperativity of 12 still cannot not solve the optimization problem. As shown in Fig. S1A (right), even if the cooperativity is increased to 12, the one-loop system requires a level of basal receptor activity, R, that needs to be both greater than 0.35 (to prevent more than 0.1% dedifferentiation) and less than 0.15 (to be able to control of the experimentally observed 0.5% rate of preadipocyte differentiation). (B) Having a multi-loop system solves the optimization problem (same Model 2 results shown in Fig. 2). The variability in Ron and Roff is actually similar for Ron and Roff, but only looks asymmetric because we are introducing lognormal noise, but are plotting R on a linear scale in Fig. S1B to better illustrate the change in PPARG values versus R. **(C)** Plotting the steady-state curves of Model 2 with R on log-scale shows that the variability in Ron and Roff is similar.

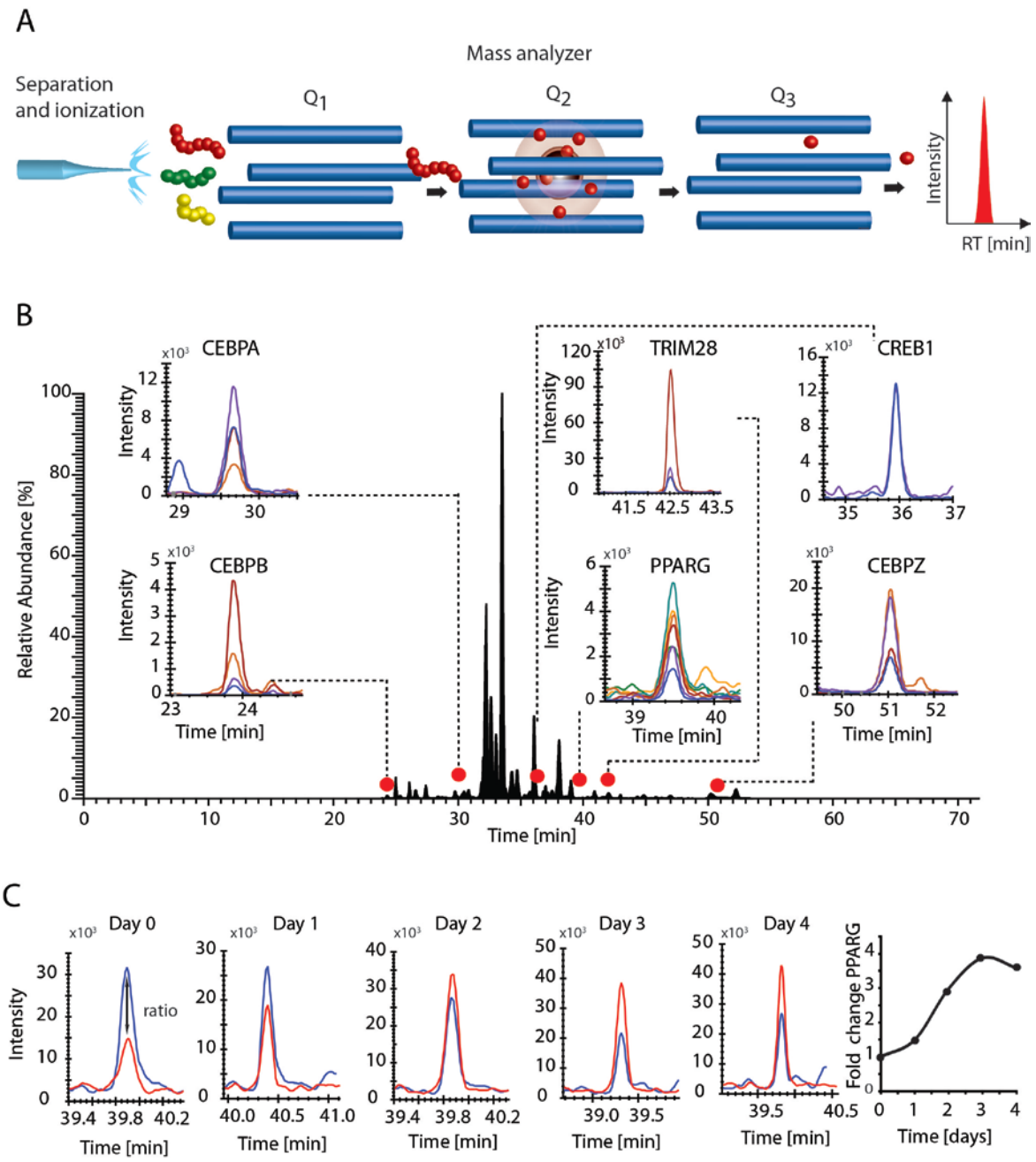

Figure S2: Development of a method to systematically uncover feedback loops in a protein network. A) Selective reaction monitoring (SRM) mass spectrometry-based protein quantification was carried out on a triple-quad mass spectrometer coupled to a nanoflow high pressure liquid chromatography (HPLC) separation device and nanospray ionization source. The 3 quadrupoles are marked as Q1, Q2, and Q3. The transitions (precursor/fragment ions) generated for each targeted peptide were read out by the detector as intensities over time. B) Total ion chromatogram showing measurements of 60 proteins during a 70 minute experiment on a single sample consisting of 4µg of total protein digest. The inset panels show chromatograms of individual monitored peptides. C) Example of how a protein is quantified over the timecourse of adipogenesis. To calculate relative changes in abundance, heavy, isotopically-labelled versions of the peptides of interest are spiked into samples at known concentration. The heavy (blue) and light, endogeneous (red) peptides are measured and ratioed at the desired time points (right).

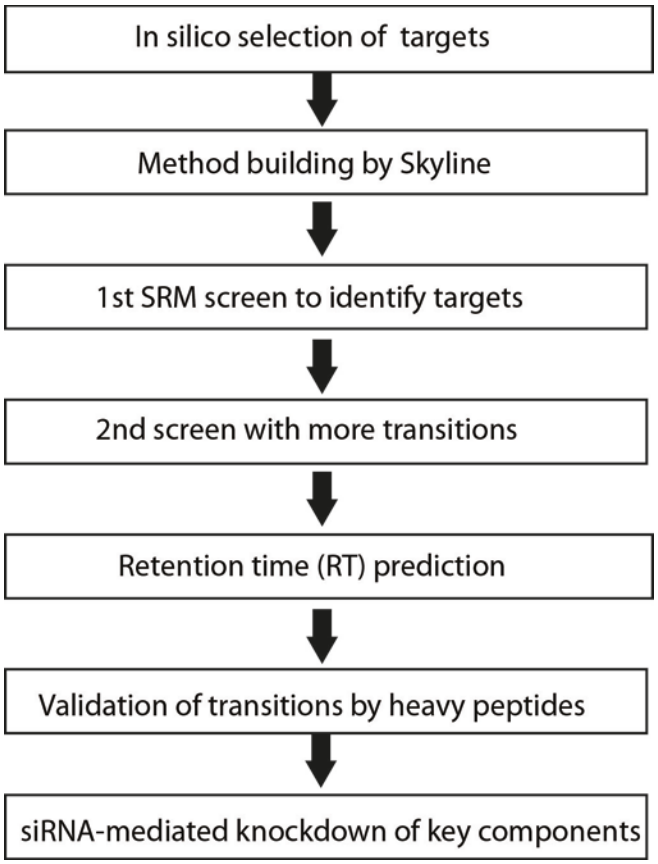

Figure S3. Workflow for developing selective reaction monitoring (SRM) mass spectrometry assays. We isolated nuclei from OP9 mouse cells. The trypsin-hydrolyzed fractions (days one and four) were used to screen for proteins of interest. Peptide signals with more than three transitions, a signal to noise ratio above 3, and transition signals that fell within the predicted retention time window (five minutes), were chosen for a second screen with up to 10 transitions. To validate the peptide transitions, heavy peptides were spiked into the sample as internal standards and analyzed by scheduled SRM. If the light (endogenous) peptide and the heavy (internal standard) displayed the same fragmentation pattern, retention time, and peak shape, then the peptide was selected for quantitative SRM. Targets of particular interest, e.g. proteins in feedback loops, were further validated by siRNA-mediated knockdown experiments.

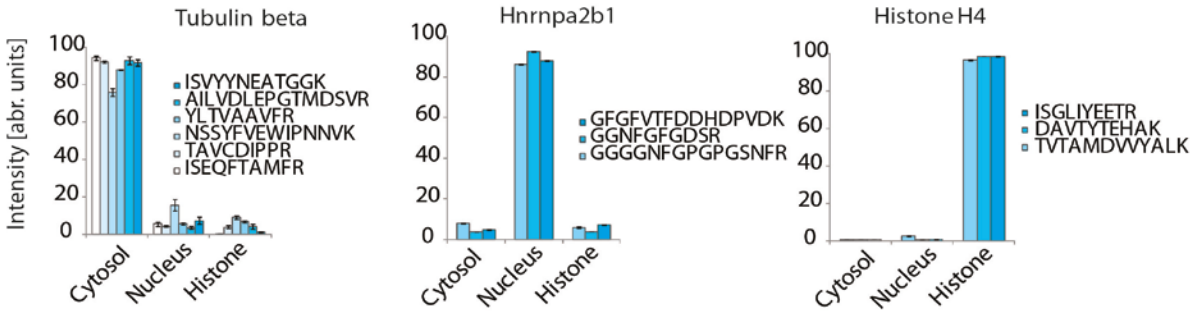

Figure S4. Verifying the specificity of the subcellular fractionation approach. Lysate from OP9 cells was separated into cytosolic, nuclear, and histone fractions and prepared for mass spectrometry analysis as per the protocol described in the Materials and Methods section. 3 µg of each fraction was analyzed using SRM-MS while monitoring the following proteins in each sample: Tubulin beta-5, HNRNPA2B1 and Histone H4, representing the Cytosol, Nucleus and Histone fractions respectively. Each datapoint is the average of 3 biological replicates (error bars show standard deviation of the mean).

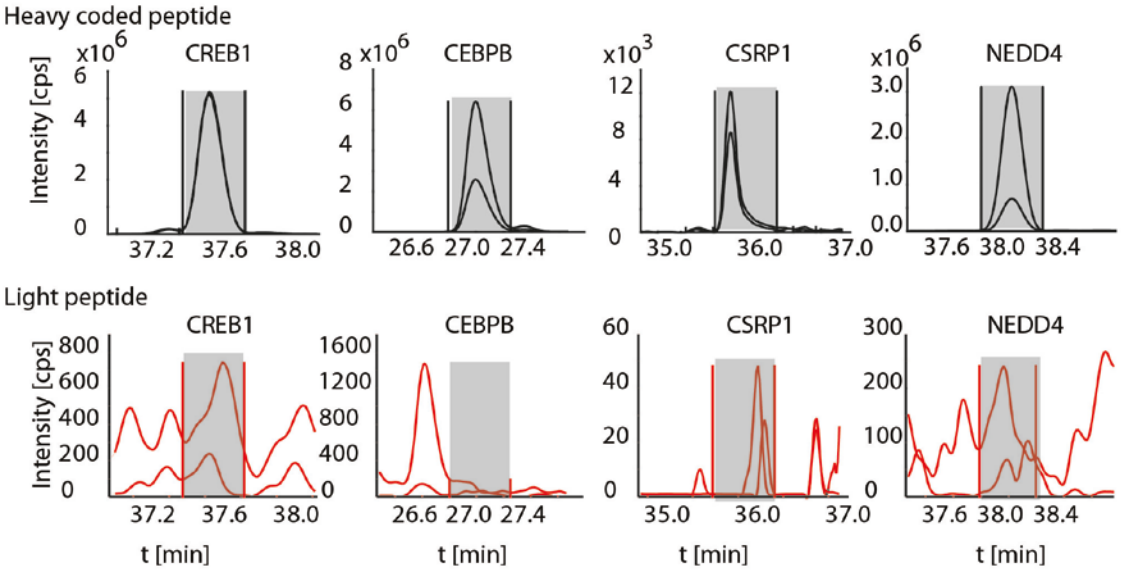

Figure S5. Background analysis of internal standard peptides. To measure the possible light background in our heavy peptide standard solution using SRM MS, 1 pmol of each heavy peptide was injected into the mass spectrometer, and light and heavy fragment ions were monitored simultaneously. The instrument was used in positive mode, and a spray voltage of 1500 V was applied. The SRM chromatograms display specific transitions for each peptide protein probe (heavy internal standard black and potential light contamination in red).

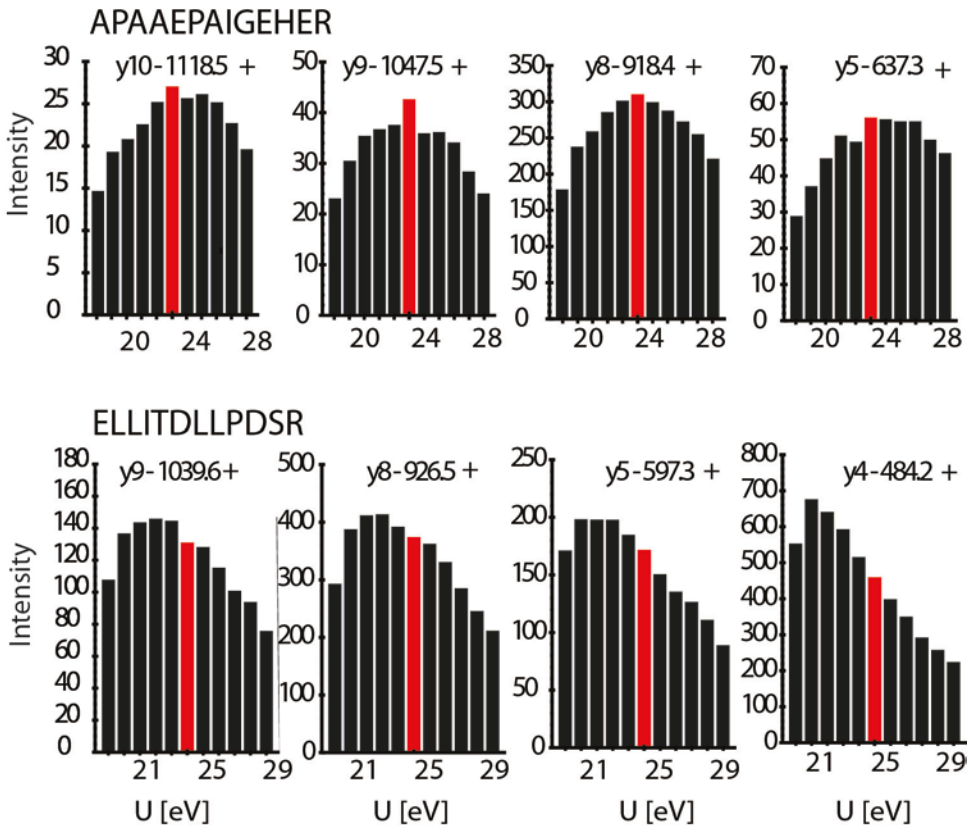

Figure S6. Optimizing collision energy for two different peptides for C/EBPB & Z. The heavy peptide is used to search for fragments with the best signal response and to optimize the collision energy for each transition to get the best possible signal to noise ratio on the TSQ Vantage triple-quadrupole mass spectrometer, the predicted collision energy for each peptide is marked in red.

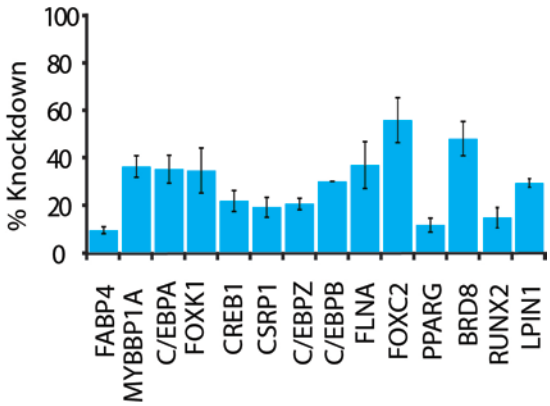

Figure S7. Using siRNA knockdown to verify the specificity of the peptides and transitions used to measure the key proteins in this study. OP9 cells were transfected with Lipofectamine and 20 nM of the individual diced pool siRNA 24 hours prior to the start of differentiation. Transfected mouse preadipocytes were treated by an adipogenic cocktail containing 0.517 µM IBMX (1-methyl-3-(2-methylpropyl)-7H-purine-2,6-dione) and 60 µM dexamethasone at the first stimulus and 172.2 nM insulin in a second stimulus over the time course of four days. The individual samples were collected and an internal standard for each monitored peptide was spiked in and the samples were measured by LC/ESI SRM MS. The obtained quantitative results were then normalized to the YFP siRNA treatment. Each datapoint is the average of 3 biological replicates (error standard deviation of the mean)

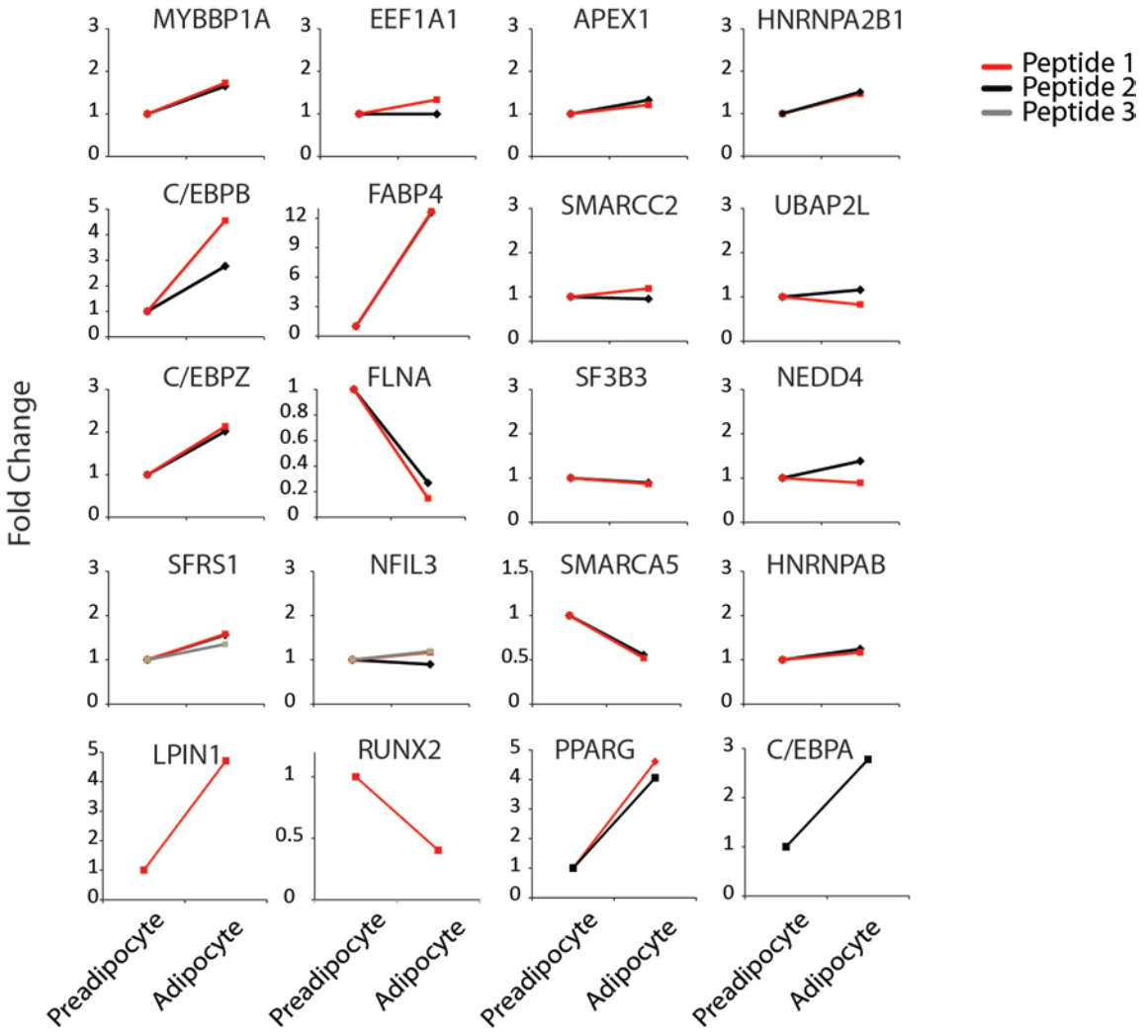

Figure S8: Multiple peptides from the same protein display the same trend during adipogenesis. To demonstrate that the selected peptides derived from one protein showed the same fold changes during differentiation, the fold change between the preadipocyte level and the adipocyte level was quantified. Samples were prepared from OP9 cells' nuclei extracted at different timepoints during adipogenesis. Heavy, isotopically-labeled peptides were spiked into each sample, and the samples were quantitatively analyzed using SRM mass spectrometry.

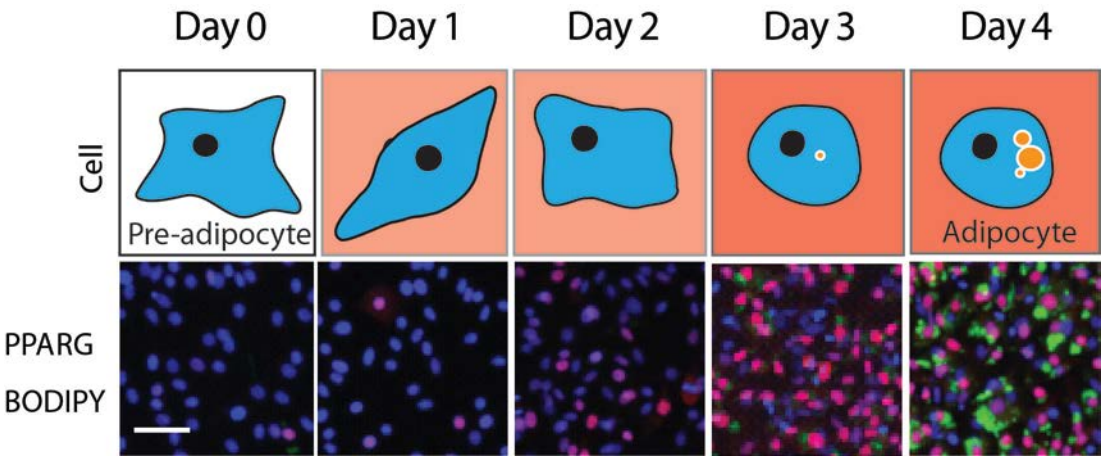

Figure S9: Quantitating protein abundance changes over the timecourse of adipogenesis using immunocytochemistry following procedures described in Park et al (7). A) Mouse OP9 preadipocyte cells were induced to differentiate by adding the standard adipogenic cocktail (DIM; 60 μM dexamethasone, 0.517 μM IBMX, and 10% FBS in MEM-α) at Day 0 and then replacing it 48 hours later with MEM-α containing 172.2 nM insulin and 10% FBS. Differentiation was monitored by measuring expression of PPARG and lipid accumulation using single-cell fluorescence imaging. Cells were stained using a specific antibody to detect PPARG (red), BODIPY 493/503 to visualize lipid droplets (green), and DAPI to stain for nuclei (blue). Scale bar, 40 μm.

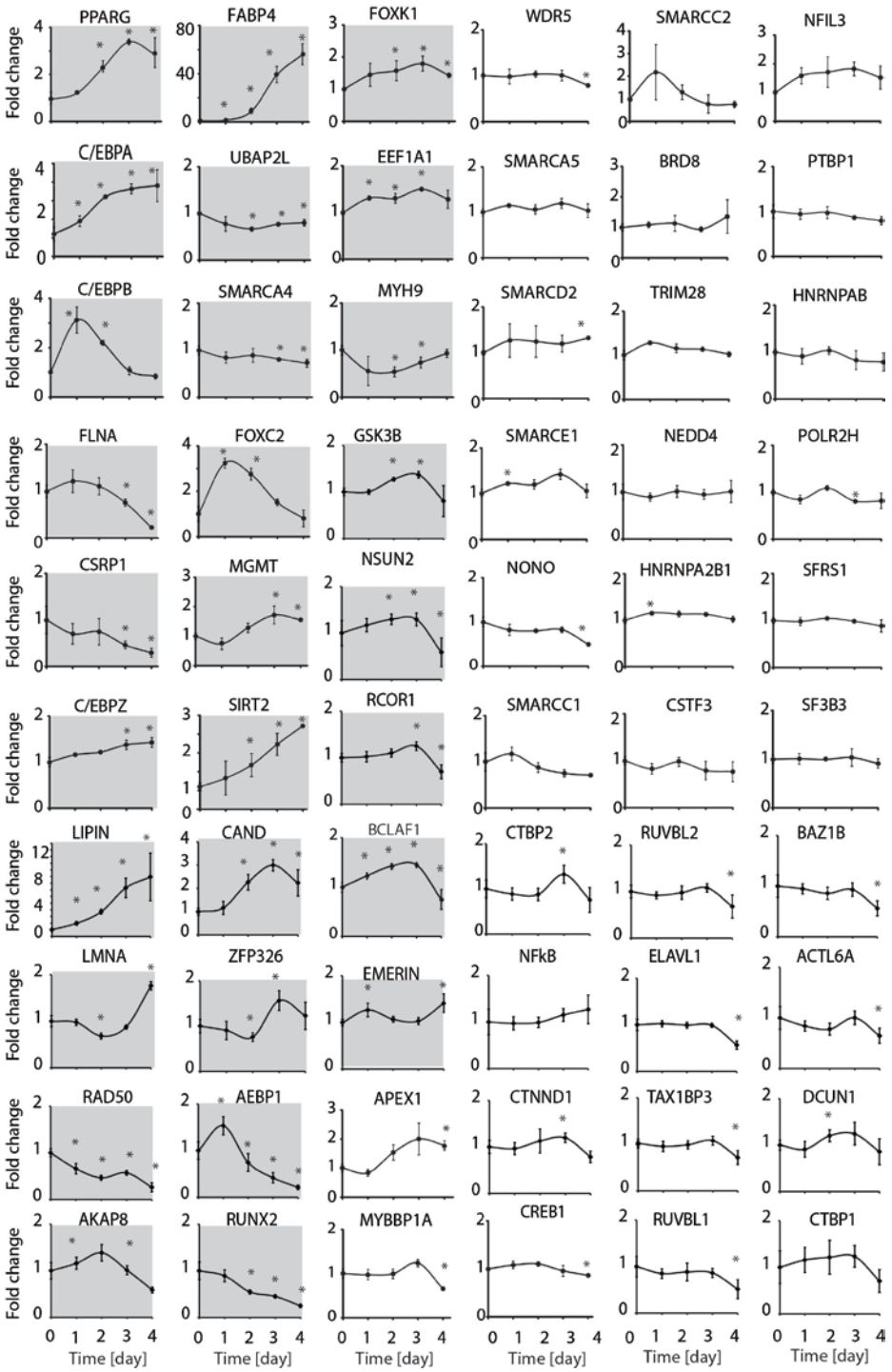

Figure S10. Quantitating protein abundance changes over the timecourse of adipogenesis using SRM mass spectrometry. Nuclear protein abundance changes were measured over the timecourse of adipogenesis Each datapoint is the average of 3 biological replicates (error standard deviation of the mean). Adipogenesis was induced using DIM. Samples were prepared from nuclei extracted from OP9 cells at different timepoints during adipogenesis. Heavy, isotopically-labeled peptides were spiked into each sample, and the samples were quantitatively analyzed using SRM mass spectrometry. A protein was classified as "changing" during adipogenesis if there was a significant difference in its abundance from the Day 0 value at least at two time points during adipogenesis, $p < 0.05$ (*). "Changing" proteins are highlighted in grey boxes. All measurements were normalized to the values at Day 0 of the differentiation timecourse.

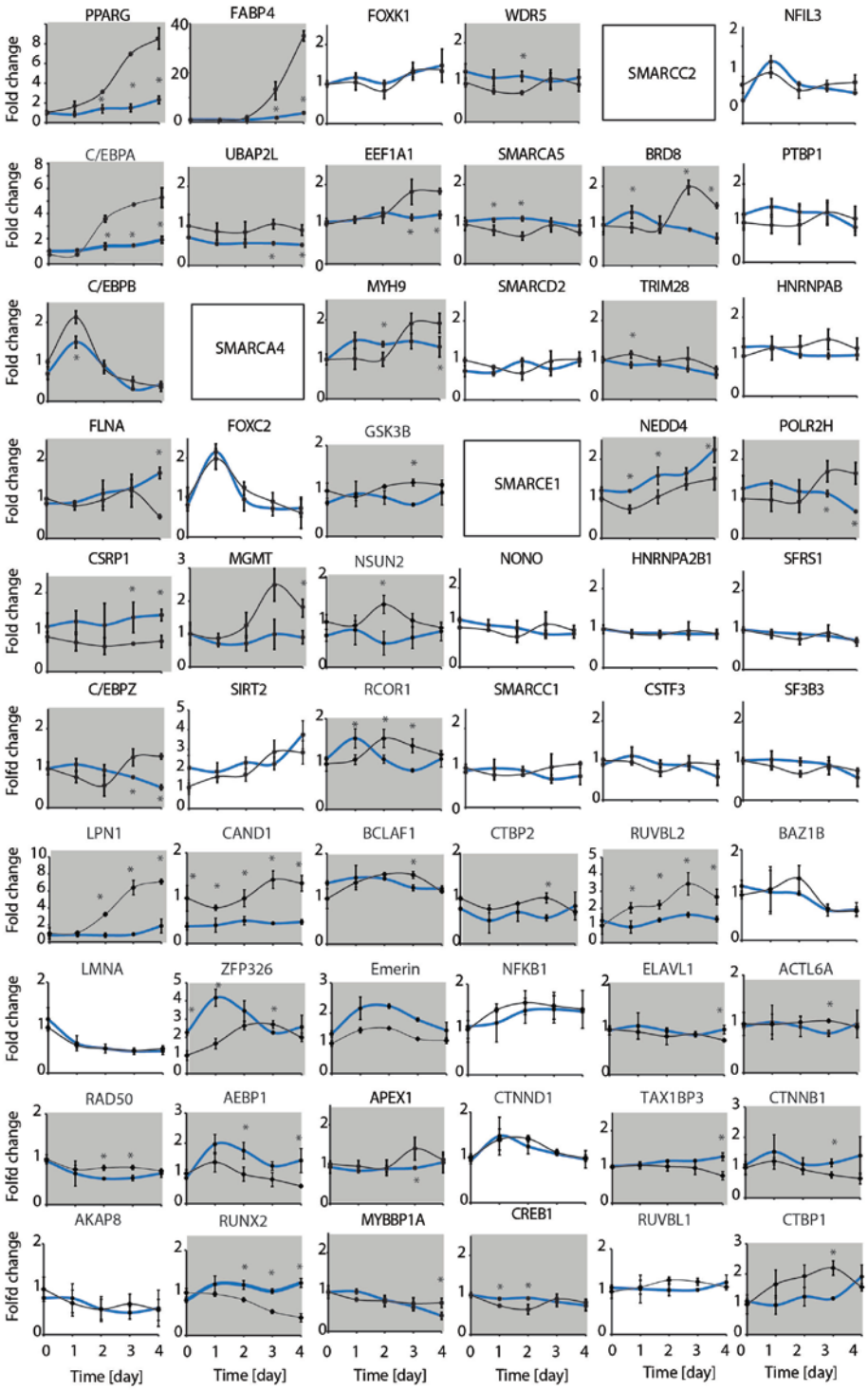

Figure S11. Testing for PPARG-regulated proteins using siRNA-mediated knockdown of PPARG expression. OP9 preadipocytes were transfected with siRNA targeting PPARG (blue) or YFP as a control (black) and then 24 hours later, were induced to differentiate by addition of the adipogenic cocktail. A protein was classified as influenced by the PPARG knockdown and highlighted by a grey box if its abundance in the PPARG knockdown versus control (YFP) samples varied significantly at one or more timepoints, $p < 0.05$ (*). "Influenced" proteins are highlighted in grey boxes. Each datapoint is the average of 3 biological replicates (error standard deviation of the mean).

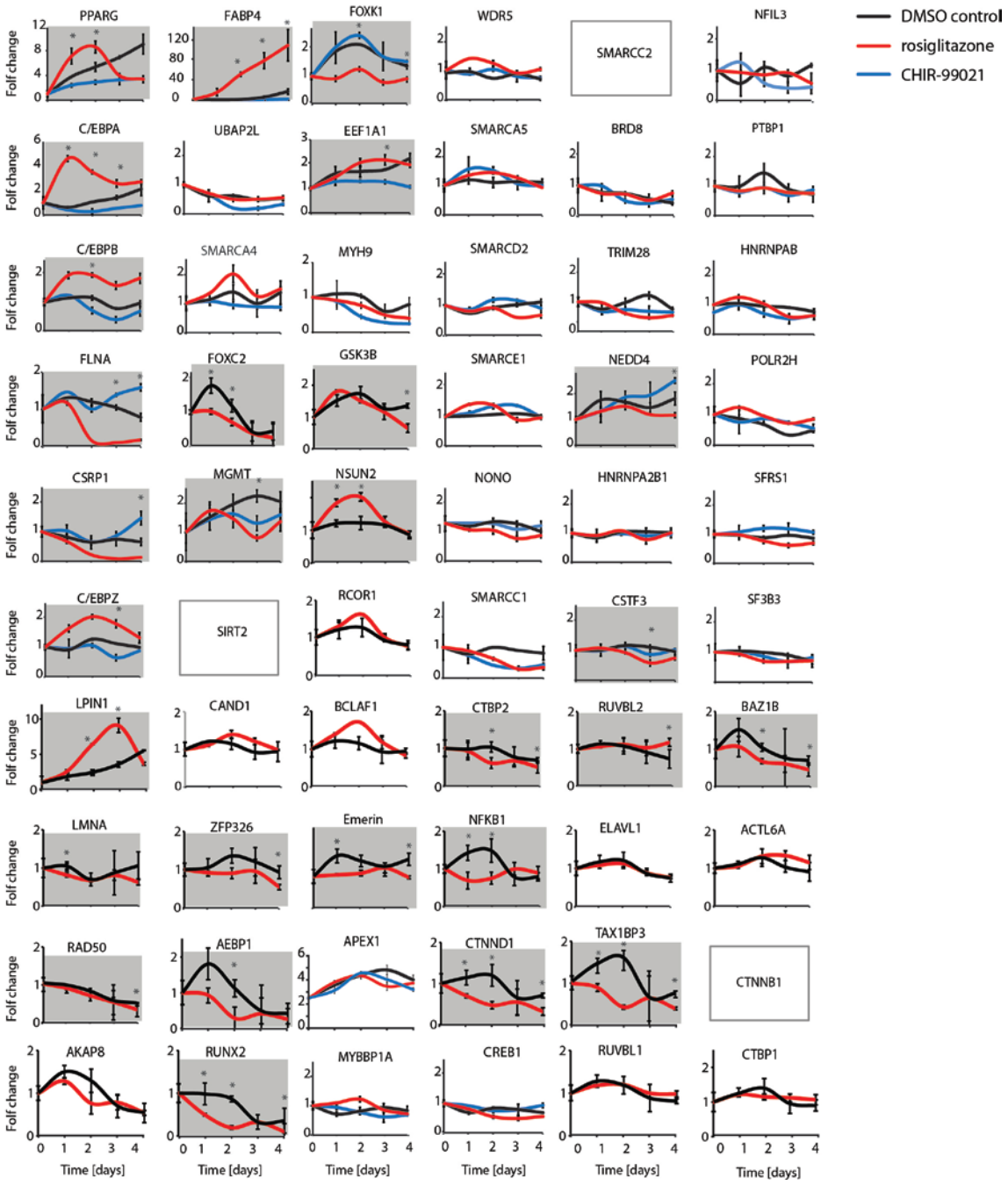

Figure S12. Validating PPARG-regulated proteins by modulating PPARG activity using chemical perturbations. PPARG activity was perturbed using small molecules. 10 µM rosiglitazone (red), 0.5 µM Chir-99021 (blue), or DMSO control (black) was added at Day 0 together with the adipogenesis-inducing stimulus (DIM). The protein was categorized as influenced by PPARG activity if it met two criteria. First, its abundance both in the PPARG-activated (rosiglitazone) sample and in the PPARG-inhibited (CHIR-99021) sample had to be significantly different from the control in at least one of the 5 time points as determined by a pairwise t-test, $p < 0.05$ (*). Second, PPARG activation and inhibition had to show opposite effects on the protein abundance compared to the control. Each datapoint is the average of 3 biological replicates (error standard deviation of the mean). “Influenced” proteins are highlighted in grey boxes.

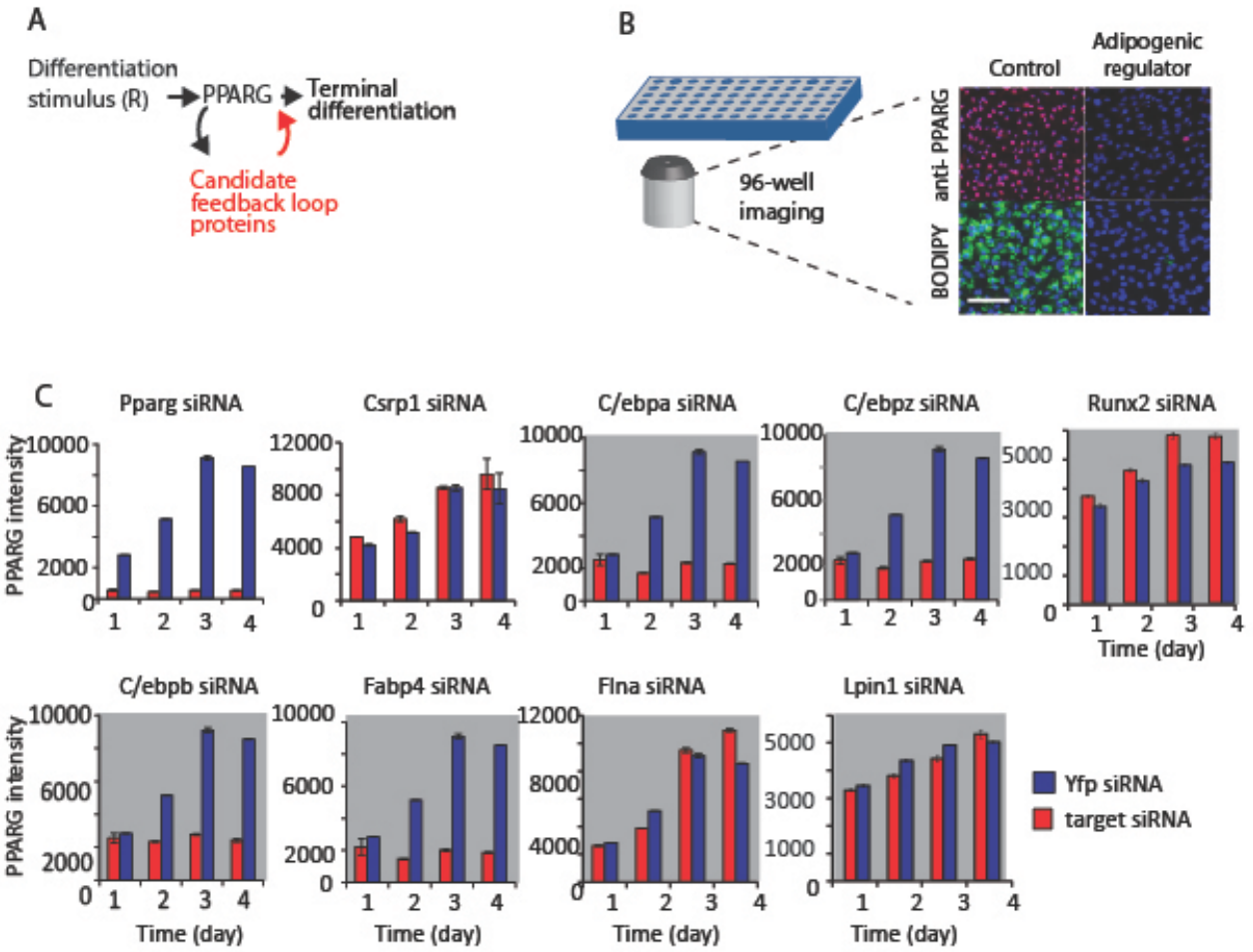

Figure S13. Using siRNA-mediated knockdown to identify regulators of PPARG. (A) Strategy to reveal which proteins can regulate PPARG. Direction of the applied perturbation is indicated by a red arrow. B) Following protocols described in Park et al. *(7)*, mouse OP9 preadipocytes were transfected with siRNA and, 24 hours later, were induced to differentiate by addition of a quarter stimulus of the adipogenic DIM cocktail. PPARG expression and lipid accumulation (BODIPY) were quantitatively measured over the timecourse of 4 days by three-color immunocytochemistry staining: PPARG (red), BODPIY(green), DAPI (blue). Images show OP9 cells at day four after induction of differentiation without (control) and with siRNA-mediated knockdown of the adipogenic regulator. Scale bar, 80 μm. C) Results of the immunocytochemistry staining. Each bar represents the average of approximately 10,000 individual cells. Error bars show standard deviation. Proteins found to be in feedback loops with PPARG are highlighted in grey boxes.

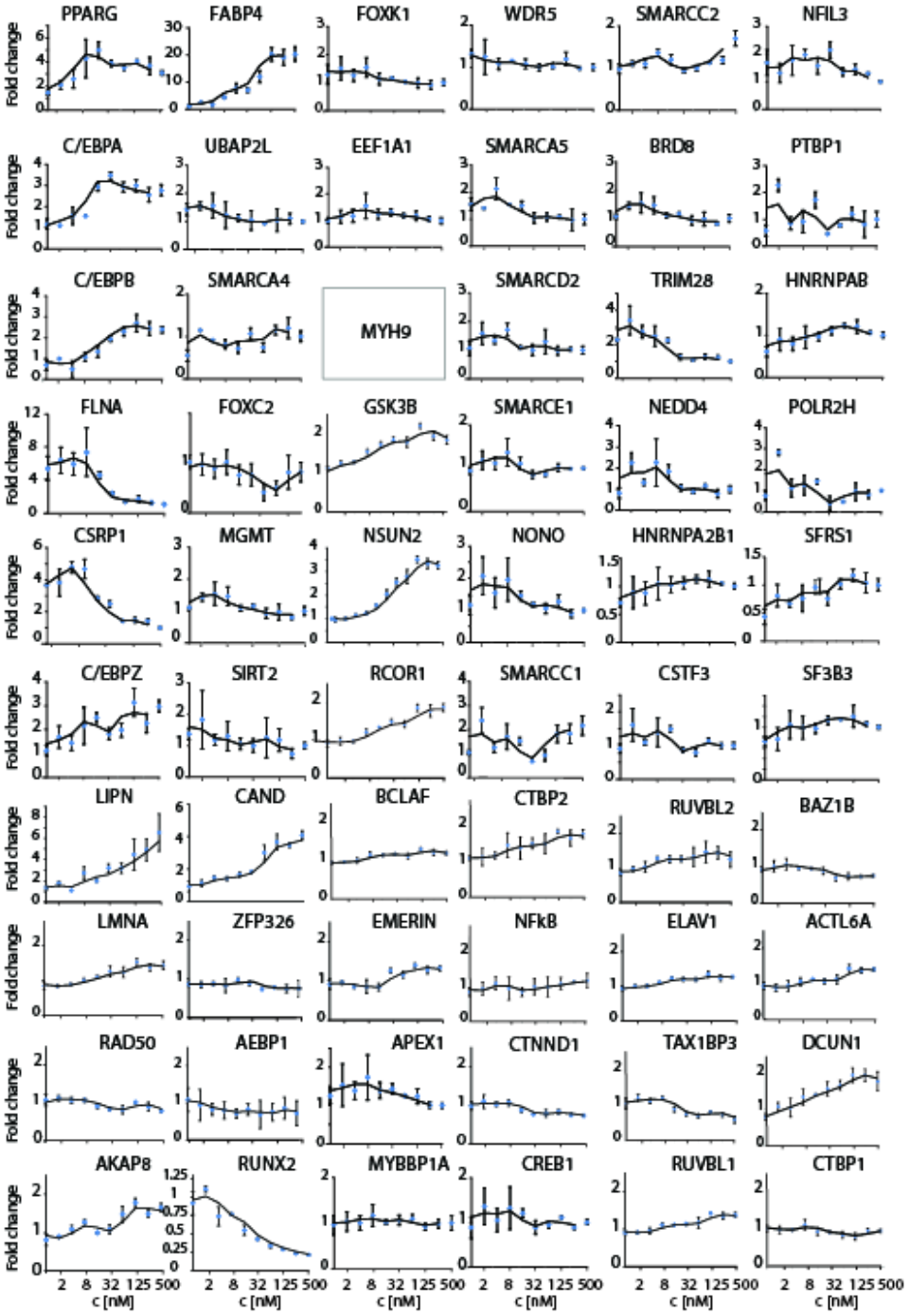

Figure S14. Titrating a chemical activator of PPARG to determine the relationship between PPARG activation and the abundance of the candidate proteins. The PPARG activator rosiglitazone was titrated into the media of undifferentiated OP9 cells, and the resulting protein expression levels were monitored after 48 hours, a timepoint at which all three main transcription factors (PPARG, C/EBPA and C/EBPB) were maximally expressed (7). A cooperative relationship is apparent between PPARG activity and expression of several proteins. Nuclear lysates were extracted, prepared, and analyzed by SRM mass spectrometry. Each datapoint is the average of 3 biological replicates (error standard deviation of the mean). The abundance of each time point was normalized to the concentration at the start or end point at 0 or 500 nM.

References and Notes

1. J. Zuber, J. Shi, E. Wang, A. R. Rappaport, H. Herrmann, E. A. Sison, D. Magoon, J. Qi, K. Blatt, M. Wunderlich, M. J. Taylor, C. Johns, A. Chicas, J. C. Mulloy, S. C. Kogan, P. Brown, P. Valent, J. E. Bradner, S. W. Lowe, C. R. Vakoc, RNAi screen identifies Brd4 as a therapeutic target in acute myeloid leukaemia. *Nature* **478**, 524–528 (2011). Medline doi:10.1038/nature10334

2. Y. D. Tchoukalova, M. G. Sarr, M. D. Jensen, *Am. J. Physiol.* **287**, R1132 (2004).

3. A. Chawla, E. J. Schwarz, D. D. Dimaculangan, M. A. Lazar, Peroxisome proliferator-activated receptor (PPAR) gamma: Adipose-predominant expression and induction early in adipocyte differentiation. *Endocrinology* **135**, 798–800 (1994). Medline

4. E. D. Rosen, C. H. Hsu, X. Wang, S. Sakai, M. W. Freeman, F. J. Gonzalez, B. M. Spiegelman, C/EBPalpha induces adipogenesis through PPARgamma: A unified pathway. *Genes Dev.* **16**, 22–26 (2002). Medline doi:10.1101/gad.948702

5. K. L. Spalding, E. Arner, P. O. Westermark, S. Bernard, B. A. Buchholz, O. Bergmann, L. Blomqvist, J. Hoffstedt, E. Näslund, T. Britton, H. Concha, M. Hassan, M. Rydén, J. Frisén, P. Arner, Dynamics of fat cell turnover in humans. *Nature* **453**, 783–787 (2008). Medline doi:10.1038/nature06902

6. G. M. Süel, R. P. Kulkarni, J. Dworkin, J. Garcia-Ojalvo, M. B. Elowitz, Tunability and noise dependence in differentiation dynamics. *Science* **315**, 1716–1719 (2007). Medline doi:10.1126/science.1137455

7. B. O. Park, R. Ahrends, M. N. Teruel, Consecutive positive feedback loops create a bistable switch that controls preadipocyte-to-adipocyte conversion. *Cell Reports* **2**, 976–990 (2012). Medline doi:10.1016/j.celrep.2012.08.038

8. H. H. Chang, M. Hemberg, M. Barahona, D. E. Ingber, S. Huang, Transcriptome-wide noise controls lineage choice in mammalian progenitor cells. *Nature* **453**, 544–547 (2008). Medline doi:10.1038/nature06965

9. J. Hanna, K. Saha, B. Pando, J. van Zon, C. J. Lengner, M. P. Creyghton, A. van Oudenaarden, R. Jaenisch, Direct cell reprogramming is a stochastic process amenable to acceleration. *Nature* **462**, 595–601 (2009). Medline doi:10.1038/nature08592

10. S. Palani, C. A. Sarkar, Transient noise amplification and gene expression synchronization in a bistable mammalian cell-fate switch. *Cell Reports* **1**, 215–224 (2012). Medline doi:10.1016/j.celrep.2012.01.007

11. A. Poloni, G. Maurizi, P. Leoni, F. Serrani, S. Mancini, A. Frontini, M. C. Zingaretti, W. Siquini, R. Sarzani, S. Cinti, Human dedifferentiated adipocytes show similar properties to bone marrow-derived mesenchymal stem cells. *Stem Cells* **30**, 965–974 (2012). Medline doi:10.1002/stem.1067

12. C. Talchai, S. Xuan, H. V. Lin, L. Sussel, D. Accili, Pancreatic β cell dedifferentiation as a mechanism of diabetic β cell failure. *Cell* **150**, 1223–1234 (2012). Medline doi:10.1016/j.cell.2012.07.029

13. T. Reiff, K. Tsarovina, A. Majdazari, M. Schmidt, I. del Pino, H. Rohrer, Neuroblastoma phox2b variants stimulate proliferation and dedifferentiation of immature sympathetic neurons. *J. Neurosci.* **30**, 905–915 (2010). Medline doi:10.1523/JNEUROSCI.5368-09.2010

14. P. R. Tata, H. Mou, A. Pardo-Saganta, R. Zhao, M. Prabhu, B. M. Law, V. Vinarsky, J. L. Cho, S. Breton, A. Sahay, B. D. Medoff, J. Rajagopal, Dedifferentiation of committed epithelial cells into stem cells in vivo. *Nature* **503**, 218–223 (2013). Medline

15. S. E. Senyo, M. L. Steinhauser, C. L. Pizzimenti, V. K. Yang, L. Cai, M. Wang, T. D. Wu, J. L. Guerquin-Kern, C. P. Lechene, R. T. Lee, Mammalian heart renewal by pre-existing cardiomyocytes. *Nature* **493**, 433–436 (2013). Medline doi:10.1038/nature11682

16. M. Niepel, S. L. Spencer, P. K. Sorger, Non-genetic cell-to-cell variability and the consequences for pharmacology. *Curr. Opin. Chem. Biol.* **13**, 556–561 (2009). Medline doi:10.1016/j.cbpa.2009.09.015

17. Q. A. Wang, C. Tao, R. K. Gupta, P. E. Scherer, Tracking adipogenesis during white adipose tissue development, expansion and regeneration. *Nat. Med.* **19**, 1338–1344 (2013). Medline doi:10.1038/nm.3324

18. N. B. Trunnell, A. C. Poon, S. Y. Kim, J. E. Ferrell Jr., Ultrasensitivity in the Regulation of Cdc25C by Cdk1. *Mol. Cell* **41**, 263–274 (2011). Medline doi:10.1016/j.molcel.2011.01.012

19. O. Brandman, J. E. Ferrell Jr., R. Li, T. Meyer, Interlinked fast and slow positive feedback loops drive reliable cell decisions. *Science* **310**, 496–498 (2005).

20. E. D. Rosen, O. A. MacDougald, Adipocyte differentiation from the inside out. *Nat. Rev. Mol. Cell Biol.* **7**, 885–896 (2006). Medline doi:10.1038/nrm2066

21. R. Berry, E. Jeffery, M. S. Rodeheffer, Weighing in on adipocyte precursors. *Cell Metab.* **19**, 8–20 (2014).

22. D. C. Berry, D. Stenesen, D. Zeve, J. M. Graff, The developmental origins of adipose tissue. *Development* **140**, 3939–3949 (2013). Medline doi:10.1242/dev.080549

23. N. E. Wolins, B. K. Quaynor, J. R. Skinner, A. Tzekov, C. Park, K. Choi, P. E. Bickel, OP9 mouse stromal cells rapidly differentiate into adipocytes: Characterization of a useful new model of adipogenesis. *J. Lipid Res.* **47**, 450–460 (2006). Medline doi:10.1194/jlr.D500037-JLR200

24. E. Abell, R. Ahrends, S. Bandara, B. O. Park, M. N. Teruel, Parallel adaptive feedback enhances reliability of the Ca2+ signaling system. *Proc. Natl. Acad. Sci. U.S.A.* **108**, 14485–14490 (2011). Medline doi:10.1073/pnas.1018266108

25. P. Picotti, B. Bodenmiller, L. N. Mueller, B. Domon, R. Aebersold, Full dynamic range proteome analysis of *S. cerevisiae* by targeted proteomics. *Cell* **138**, 795–806 (2009). Medline doi:10.1016/j.cell.2009.05.051

26. M. I. Lefterova, Y. Zhang, D. J. Steger, M. Schupp, J. Schug, A. Cristancho, D. Feng, D. Zhuo, C. J. Stoeckert Jr., X. S. Liu, M. A. Lazar, PPARγ and C/EBP factors

orchestrate adipocyte biology via adjacent binding on a genome-wide scale. *Genes Dev.* **22**, 2941–2952 (2008). Medline doi:10.1101/gad.1709008

27. S. D. Ayers, K. L. Nedrow, R. E. Gillilan, N. Noy, Continuous nucleocytoplasmic shuttling underlies transcriptional activation of PPARgamma by FABP4. *Biochemistry* **46**, 6744–6752 (2007). Medline doi:10.1021/bi700047a

28. H. E. Kim, E. Bae, D. Y. Jeong, M. J. Kim, W. J. Jin, S. W. Park, G. S. Han, G. M. Carman, E. Koh, K. S. Kim, Lipin1 regulates PPARγ transcriptional activity. *Biochem. J.* **453**, 49–60 (2013). Medline doi:10.1042/BJ20121598

29. P. Tontonoz, B. M. Spiegelman, Fat and beyond: The diverse biology of PPARgamma. *Annu. Rev. Biochem.* **77**, 289–312 (2008). Medline doi:10.1146/annurev.biochem.77.061307.091829

30. T. Galvez, M. N. Teruel, W. D. Heo, J. T. Jones, M. L. Kim, J. Liou, J. W. Myers, T. Meyer, siRNA screen of the human signaling proteome identifies the PtdIns(3,4,5)P3-mTOR signaling pathway as a primary regulator of transferrin uptake. *Genome Biol.* **8**, R142 (2007). Medline doi:10.1186/gb-2007-8-7-r142

31. J. R. Taylor, *An Introduction to Error Analysis: The Study of Uncertainties in Physical Measurements* (University Science, Sausalito, CA, ed. 2, 1997).